Atmósfera 39, 1-32 (2025)
https://doi.org/10.20937/ATM.53358

Satellite-based analysis of climate oscillations: Implications for precipitation in an arid watershed in Mexico

David Eduardo GUEVARA-POLO[1]*, Carlos PATIÑO-GÓMEZ[1],
Martín José MONTERO-MARTÍNEZ[2] and Regina MIJARES-FAJARDO[1]

[1] *Departamento de Ingeniería Ambiental, Universidad de las Américas Puebla, 72810 San Andrés Cholula, Puebla, México.*
[2] *Subcoordinación de Eventos Extremos y Cambio Climático, Instituto Mexicano de Tecnología del Agua, Paseo Cuauhnáhuac 8532, Colonia Progreso, 62550 Jiutepec, Morelos, México.*
*Corresponding author; email: david.guevarapo@udlap.mx

Received: November 17, 2023; Accepted: July 29, 2024

RESUMEN

Se sabe que las oscilaciones climáticas tienen una influencia importante en patrones meteorológicos en todo el mundo. Mientras que el impacto de El Niño Oscilación del Sur (ENSO) está muy bien documentada, los estudios que examinan los efectos de la Oscilación Decadal del Pacífico (PDO) y la Oscilación Multidecadal del Atlántico (AMO) son limitados. Este estudio utiliza datos satelitales para confirmar que ENSO influye de manera significativa ($\alpha = 0.01$) en la precipitación en la cuenca Nazas-Aguanaval durante el periodo octubre-marzo, como lo demuestran los coeficientes de correlación de Spearman. En contraste, la influencia de la PDO se registró durante meses específicos (enero, marzo, noviembre y diciembre), en tanto que AMO impacta la precipitación durante abril-junio, noviembre y diciembre. Estos resultados se corroboraron utilizando ANOVA, reforzando la evidencia en favor del impacto de ENSO e indicando un impacto limitado de PDO y AMO en esta cuenca. Finalmente, se desarrolló un modelo de regresión lineal para estimar anomalías mensuales de precipitación basadas en la fase de estos tres índices para las distintas subcuencas. Notablemente, las anomalías se encontraron en el rango de 140 a –78% en meses de la temporada seca. Los resultados demuestran la influencia de las oscilaciones climáticas en la precipitación en la cuenca Nazas-Aguanaval y la utilidad de los datos satelitales para conducir estos análisis. Igualmente, se establece un punto de partida para investigar las implicaciones de las fases de las oscilaciones climáticas para la administración del agua y la prevención de desastres causados por sequías.

ABSTRACT

Climate oscillations are known to have an important influence on weather patterns across the world. While the impact of El Niño Southern Oscillation (ENSO) has been well documented, there is a scarcity of studies examining the effects of the Pacific Decadal Oscillation (PDO) and the Atlantic Multidecadal Oscillation (AMO). This study uses satellite data to confirm that ENSO significantly influences precipitation in the Nazas-Aguanaval watershed from October to March, as evidenced by Spearman correlation coefficients. In contrast, the PDO influence is registered during specific months (January, March, November and December), while AMO impacts precipitations during April-June, November, and December. These results were corroborated using ANOVA, reinforcing the influence of ENSO and indicating a limited impact of PDO and AMO on this watershed. Finally, a linear model was developed to estimate monthly precipitation anomalies based on the phase of these three indices for the different sub-basins. Notably, monthly precipitation anomalies ranged between 140% and –78% in dry months. Our results demonstrate the influence of climate oscillations in precipitation in the Nazas-Aguanaval watershed and the usefulness of satellite data for conducting these analyses. Likewise, we set a starting point for investigating the implications of climate oscillation phases for water management and drought disaster prevention.

Keywords: teleconnections, climate oscillations, El Niño Southern Oscillation, Pacific Decadal Oscillation, Atlantic Multidecadal Oscillation, precipitation.

1. Introduction

Climate variability, characterized by long-term fluctuations in the average state of the climate, can be seen at different time scales, such as month to month (intraseasonal), year to year (interannual), or decade to decade (decadal). One manifestation of this variability is climate oscillations, periodic variations in air temperature, sea surface temperature, atmospheric pressure, or precipitation compared to their average state. Some examples of climate oscillations include the El Niño Southern Oscillation (ENSO), the Pacific Decadal Oscillation (PDO), and the Atlantic Multidecadal Oscillation (AMO).

These oscillations are described using climate indices, time series that treat statistically raw measurements of climate variables. ENSO has been described using different climate indices such as Multivariate ENSO Index (MEI), Oceanic Niño Index (ONI), El Niño 3.4, and Southern Oscillation Index (SOI). MEI is based on six meteorological variables, while SOI deals with sea level pressure, and ONI and El Niño 3.4 use sea surface temperature (SST) (Van-Viet, 2021). Similarly, PDO and AMO deal with SST in the North Pacific and the North Atlantic, respectively.

The manifestation of climate oscillations, such as ENSO, can result in teleconnections and links between climate variables from geographically distant regions (Nigam and Baxter, 2015). In this sense, there may be a correlation between the status of climate indices and precipitation. In Mexico, the influence of ENSO on interannual precipitation variability has been well documented, with a significant impact observed at the national and local scales (Magaña et al., 2003; Bhattacharya and Chiang, 2014). A recent review has shown that the positive (negative) phase of ENSO in Mexico produces wet (dry) conditions in the northern region during both summer and winter. In contrast, the opposite is observed in the center and south, with dry (wet) conditions in the summer (Guevara-Polo and Mijares-Fajardo, 2021). This type of behavior has been demonstrated in other studies in the country (Méndez and Magaña, 2010; Montero-Martínez et al., 2018).

The study of ENSO's impact on rainfall in Mexico has progressed, and recent research has provided further insights. For instance, by March 2024, there was a 55% chance of La Niña developing during the rainy season of 2024, which may produce negative rainfall anomalies in most of the Mexican territory (Torres, 2024). ENSO influences winter precipitation across most regions of Mexico (Álvarez-Olguín and Escalante-Sandoval, 2017). These effects have been studied regionally; for example, in the Altiplano, droughts have been associated with the negative phase of ENSO (La Niña) (Vega-Camarena et al., 2023), while El Niño is related to wet periods in northern Mexico (Mijares-Fajardo et al., 2023).

Although it is the most studied, ENSO is not the only phenomenon that affects Mexico. A recent study that employed weather stations across the country reported that PDO, AMO, and NAO also influence precipitation patterns in Mexico with different magnitudes according to the season and the region (Álvarez-Olguín and Escalante-Sandoval, 2017). For example, in Central Mexico, marked dryness was mostly associated with the co-occurrence of highly positive PDO and negative AMO between ~1600 and 1900 (Park et al., 2017). Also, recent studies in northern Mexico have reported the influence of AMO and PDO in precipitation (Llanes-Cárdenas et al., 2020; Mijares-Fajardo et al., 2023). In the Altiplano, rainfall occurrence is not subjected only to ENSO but to the combination of AMO and PDO because when the former is positive and the latter is negative or neutral, rainfall is above average and when both are negative, drought happens (Vega-Camarena et al., 2023). These three climate indices are considered in this study.

These manifestations of climate variability can reduce surface and groundwater availability, therefore compromising water security, a crucial dimension of human security. Teleconnections can significantly impact precipitation patterns and, in turn, the availability of renewable water resources. Understanding the teleconnections between climate oscillations and precipitation can inform water management decisions and support drought prevention and mitigation

measures. Mexico is a country particularly vulnerable to these phenomena, and the Nazas-Aguanaval watershed, located in the high plains of Mexico, is no exception.

The Nazas-Aguanaval watershed is crucial for several reasons. It accounts for 20% of the national milk production and is the leading region for melon and sorghum production (Ramírez Barraza et al., 2019). It also hosts the irrigation district with the highest number of users, an aquifer ranked in the 3rd percentile for insufficient water availability, and a metropolitan area with more than 1.4 million inhabitants. Moreover, this watershed is representative of arid and semi-arid conditions, which cover two-thirds of Mexican territory.

To investigate the presence of teleconnections, observational data from surface stations is commonly analyzed to compute the correlations between climate indices and precipitation. However, the use of satellite data has been increasing in hydrological and meteorological studies to enhance our understanding of precipitation patterns. Recent studies have shown that satellite-based precipitation estimates can make reasonably complete data available, better measurements of precipitation, and improve our understanding of the hydrological cycle (Levizzani and Cattani, 2019). These data sources are useful for regions where ground data is scarce, not publicly available, or does not have enough quality. Mexico is an example where some of these conditions are present. However, although these databases are widely available and easily downloaded, confirmation of their validity in the study areas of interest is worth making.

Identifying the influence of climate oscillations on water availability is relevant for informing water management actions. In Central Mexico, a study was conducted to assess the influence of climate oscillations on surface water availability (Silva-Aguilera et al., 2024). Such studies are particularly important in arid regions like the Nazas-Aguanaval watershed. Recently, in this watershed, an irrigation optimization model that uses the link between ENSO and water availability was developed (Sánchez et al., 2018). This link was improved recently using reconstructed precipitation and runoff data (Villanueva-Díaz et al., 2022).

Analysis of variance (ANOVA) has been used to observe statistically significant differences in climate sciences. There are precedents in applying successfully this statistical method in Mexico for determining statistically significant differences between observations of climate variables across surface stations (Sánchez et al., 2012; Bravo et al., 2014; Norzagaray-Campos et al., 2016).

This study aims (1) to answer whether using satellite data in studying precipitation in the Nazas-Aguanaval watershed is effective and reliable; (2) to identify teleconnections of precipitation with ENSO, PDO, and AMO in the Nazas-Aguanaval watershed; (3) to determine which climate oscillation influences the most in this watershed, and (4) to describe the monthly precipitation anomaly associated to these climate oscillations. This study adopted a watershed scale to provide valuable meteorological information for informed water management decisions. This approach has been used previously in a small basin in Central Mexico (Montero-Martínez et al., 2022).

We first outline the process for collecting and preparing the data from surface stations. Next, we compare the data obtained from surface stations with satellite data by creating representative monthly precipitation time series. Finally, we calculate the correlations between monthly precipitation and climate indices for three climate oscillations: ENSO, PDO, and AMO. Our results provide valuable insights into the understanding of climate variability in Mexico and its significance for water management.

2. Methods

2.1 Description of the study area

The study area is the 36th hydrologic region of Mexico (Nazas-Aguanaval river), displayed in Figure 1. This hydrologic region is important because it hosts the 10th most populated metropolitan area in Mexico, with 1.4 million inhabitants in 2020; an irrigation district with 33 360 users, the greatest number in the country, and 65 611.9 ha of irrigation area. This watershed can be divided into five sub-basins that exhibit distinct climate and hydrological behavior. These sub-basins can be encompassed by two watersheds, Nazas and Aguanaval, both of which are endorheic and discharge into the lowland within the Nazas-Aguanaval watershed. The former discharges to the Mayran Lagoon and the latter to the Viesca Lagoon. The sub-basins were delimited according to existing hydraulic and hydrometric infrastructure.

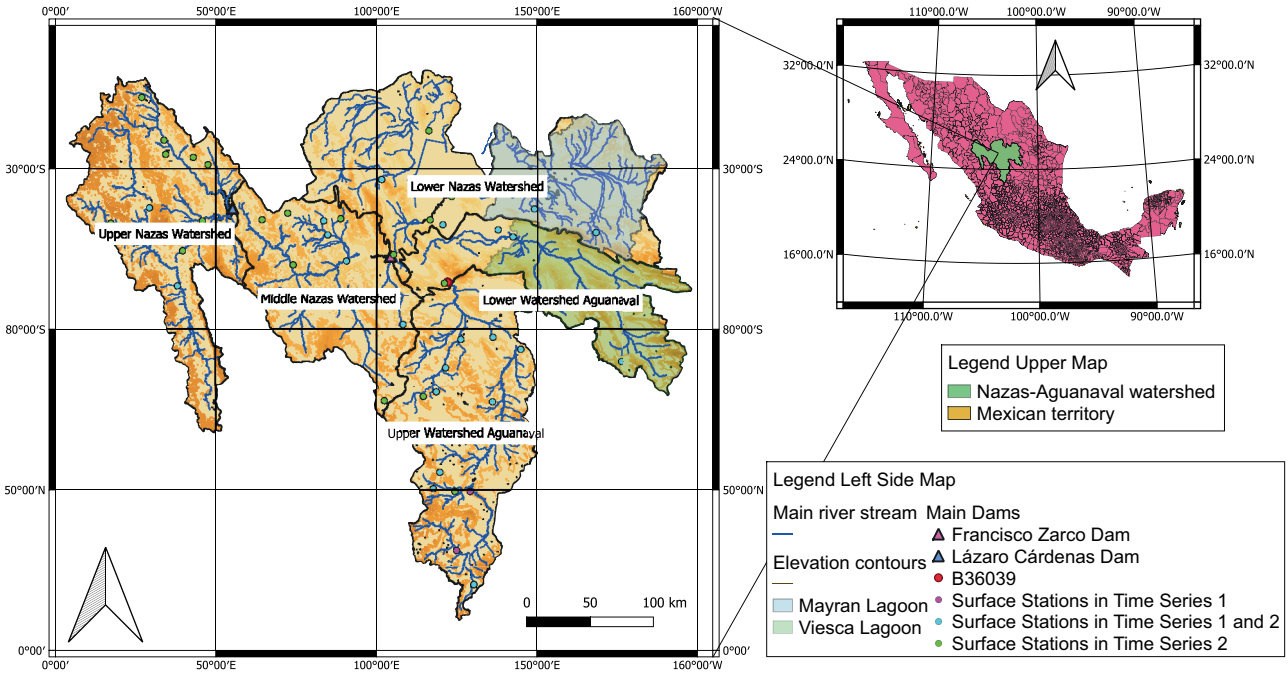

Fig. 1. Location of the Nazas-Aguanaval watershed in Mexico. Background colors on the watershed map indicate elevations, with bolder colors representing higher elevations (own elaboration based on geographic data from government agencies in Mexico).

The upper Nazas watershed ends in the Lázaro Cárdenas reservoir, the middle Nazas ends in the Francisco Zarco dam, and the lower Aguanaval watershed ends in the hydrometric station B36039. The Climate Hazards Group InfraRed Precipitation with Station Data (CHIRPS) satellite database recorded mean annual precipitations of 556, 395, and 261 mm for the upper, middle, and lower Nazas, respectively, during the most recent climatological period (1991-2020) (SG, 2024). Meanwhile, the upper and lower Aguanaval recorded 395 and 298 mm, respectively (Fig. 1).

2.2 Comparison of observational and satellite data

Monthly climate data was recovered from the public database of CONABIO (2001). The hydrologic region has 109 surface stations. To obtain the first representative precipitation time series, stations with less than 30 years of records were omitted, yielding 68 stations. Next, only stations with observations made after 1979 were selected because MEI data is available after this year. After this step, 40 stations were removed, and 28 were preserved. A period of 30 years between 1979 and 2008 was considered because it had 92.39% of data, to reduce the amount of data to be recovered.

The full watershed was considered for this comparison to allow more surface stations to be considered in the analysis and to retrieve more spatially dispersed data. Additionally, comparing the correlations of satellite-based precipitation data with climate oscillations of the entire watershed against those of sub-basins required validation, making the use of the complete watershed area necessary.

To estimate missing values in precipitation data series, a technique originally developed for an indefinite number of stations, named normal ratio method, was used (Muluken, 2020; Nadiatul and Hannani, 2021) considering three stations as follows:

$$P_4 = \frac{1}{3}\left[\frac{N_4}{N_1}P_1 + \frac{N_4}{N_2}P_2 + \frac{N_4}{N_3}P_3\right] \quad (1)$$

where P4 represents the estimated precipitation value while P1, P2, and P3 describe observed precipitation values in nearby stations. Similarly, N1, N2, and N3 represent observed annual mean precipitation in the corresponding stations.

A series of criteria was used to select the stations from which missing precipitation values were to be estimated. The first criterion was the geographic proximity to the incomplete data stations. However, 25 out of 84 pairs of stations were circularly referencing each other because of coincidental gaps in their data records. The second criterion was substituting incomplete stations in these circular reference pairs with stations with the highest correlations. In cases where this substitution was not feasible due to new circular references emerging, alternative stations with similar altitudes and horizontal distances were selected. Lastly, in cases where none of the previous criteria could be applied, the number of stations included in Eq. (1) 1 was reduced.

Total monthly values completed using this technique were 565. Given that the dataset has 10 080 monthly precipitation values (28 stations times for 360 months), modified data represented 5.61% of the total data. Even though they are a minor fraction, ANOVA was used to verify that this new data did not modify the variance of the unmodified dataset. For this analysis, a level of significance of 0.01 was considered.

Generally, in the design of experiments, the intention is to determine if a treatment has a statistically significant effect by comparing two datasets. In this way, the null hypothesis is that the treatment does not have a statistically significant effect on studied subjects. In this case, the null hypothesis was that the statistical treatment of data did not affect the natural variance of precipitation data. Once the complete dataset was computed, the representative time series was computed using the Thiessen polygon method.

A second time series for the 1979-2008 period was created to gain more spatial coverage at the expense of lower temporary coverage. The new criterion required each station to have at least 26 years of records, with missing data from up to four years estimated using Eq. (1). This meant that a maximum 13.33% of the records was to be estimated for every station. This allowed 46 surface stations in the hydrologic region to contribute with 16 560 precipitation data points, a 64.28% increase from the first time series. ANOVA was performed and Thiessen polygons were generated to compute average precipitation in the watershed. Therefore, a computation of two time series using observational data was done. The first considers 28 stations, and the second 46 stations, which will be referred to in the text as time series 1 and 2.

Time series 3 was derived using satellite data. Daily data was recovered from the CHIRPS database (SG, 2024) for the period 1981-2021 (40 years) and the total monthly precipitation was computed. Among satellite precipitation products, CHIRPS has proven to be one of the most accurate in Mexico (Rincón-Ávalos et al., 2022). This data source has been successfully used for hydrological purposes in the arid Mexico high plains near the study area (Hernández-Romero et al., 2022), as well as hydrogeological purposes (González-Ortigoza et al. 2023). In addition, it can be applied to climatological studies (Perdigón-Morales et al., 2019) and, under certain conditions, to extreme events (Villate et al., 2023). This database directly computes the average precipitation in the watershed using a geoJSON file.

The time series were compared using Pearson, Kendall, and Spearman correlations. Considering that Pearson's correlations are parametric, a Shapiro-Wilk test was performed for the 12 monthly datasets and for the annual dataset, where the null hypothesis is that the data is normally distributed. Afterward, a Box-Cox transformation was used to convert the monthly datasets where there was evidence to reject the null hypothesis, and the Shapiro-Wilk test was repeated. The level of significance was defined as 0.05. Spearman and Kendall correlations were computed without the Box-Cox transformation since they do not assume that the distribution of data is normal.

2.3 Spearman correlations

Spearman correlations were selected to study teleconnections between climate indices (ENSO, PDO, and AMO) and monthly precipitation data in the Nazas-Aguanaval watershed. The Spearman method has been proven to be effective in northern Mexico (Mijares-Fajardo et al., 2023). ENSO was described using the MEI, the Oceanic Nino Index (ONI), and the Nino3.4 to compare the use of different indices. Finally, PDO and AMO were also studied to compare their influence with ENSO's in the Nazas-Aguanaval region. Links to databases for MEI, ONI, Niño 3.4, PDO, and AMO are reported in Table I. The MEI, ONI, PDO, and AMO datasets were paired with monthly precipitation data. For the bimonthly report-

Table I. Climate indices database sources.

Index	Reference
MEI	NOAA (2024c)
ONI	NOAA (2024a)
Niño 3.4	NOAA (2024d)
PDO	NOAA (2024e)
AMO	NOAA (2024b)

ed MEI, where values are given for pairs of months (for example, January and February), the data was paired with the precipitation of the second month (for example, the January-February MEI value was paired with February precipitation). Similarly, for the trimonthly reported ONI, the index value was paired with the precipitation of the first month (for example, the January-February-March index was paired with the January precipitation value). Niño 3.4, PDO, and AMO are reported monthly. It is important to note that these are zero-lag correlations.

2.4 Monthly ANOVA

Three climate oscillations are considered in this study as the factors that affect precipitation: ENSO, AMO, and PDO. After reviewing the performance of the different ENSO indices in the correlation analysis, the ANOVA focused on just one index. The climate index used to describe ENSO is MEI due to its composite nature that incorporates six different variables. Moreover, its signal on precipitation has been observed for more months in the study area (Villanueva-Díaz et al., 2022). According to its phase, MEI has three possible levels that were accordingly standardized: values greater than or equal to 0.5 are assigned with the number 1, values less than or equal to –0.5 are assigned with the number –1, and values in between are assigned a value of 0.0. They describe the El Niño, La Niña, and neutral phases of ENSO, respectively. AMO and PDO are both assigned with –1.0 for the negative phase (≤ 0.0) and 1.0 for the positive phase (> 0.0). The levels for every climate oscillation were assigned according to the mathematical definition of the indices (Mantua et al., 1997; Enfield et al., 2001; McCabe et al., 2004; MacDonald and Case, 2005). Also, given that PDO and AMO have greater periodicity than ENSO it is convenient to average their states in two phases. The response variable is monthly precipitation.

The observational unit is the month for every year of the period 1981-2021. The values of precipitation were assigned according to their occurrence in the different months and phases of the climate indices. The Nazas-Aguanaval watershed shows a dry period from October to May and a wet season between June and September. Out of the 41 years in the period, 12 were predominantly neutral/La Niña, 10 were El Niño/neutral, six La Niña, five were neutral, four were El Niño, three were El Niño/La Niña, and one was El Niño/neutral/La Niña.

The statistical model for the ANOVA was proposed as follows:

$$P_{it} = \bar{P} + \Delta P_i + \varepsilon_{it} \tag{2}$$

where P_{it} represents monthly precipitation, the mean monthly precipitation, ΔP the effect of the climate index to be studied (precipitation anomaly), i its phase (from 1 to 3 for ENSO; from 1 to 2 for PDO and AMO), t the observation for the phase i, and ε_{it} the error variable, which follows a normal distribution with zero mean. The values of the variance (σ2) are mutually independent. Three different climate indices will be studied; hence, three subsets of equations describe monthly precipitation.

The null hypothesis of the ANOVA test for ENSO was established as follows:

$$\boldsymbol{H}_0\colon \Delta P_1 = \Delta P_2 = \Delta P_3 \tag{3}$$

$$\boldsymbol{H}_1\colon \Delta P_i \neq \Delta P_j; i \neq j,\ i;\ j \in [1,2,3] \tag{4}$$

Thus, the null hypothesis states that the mean response of precipitation is equal disregarding the phase of MEI. Physically, this represents that the climate oscillation does not influence precipitation amounts in the watershed in a statistically significant way. Conversely, for PDO and AMO, the null hypothesis was established as follows:

$$\boldsymbol{H}_0\colon \Delta P_1 = \Delta P_2 \tag{5}$$

$$\boldsymbol{H}_1\colon \Delta P_1 \neq \Delta P_2 \tag{6}$$

As expected, precipitation data does not follow a normal distribution, as confirmed by the Shapiro-Wilk test with a p-value of less than 2.2e06. However, the ANOVA test assumes that the outcome variable is normally distributed and has equal variances among groups (Blanca et al., 2017). To address this, we performed a Box-Cox transformation on the precipitation data. Following this transformation, the Shapiro-Wilk test yielded a p-value of 0.138, indicating that the data can now be considered as normally distributed. This transformation is important for ensuring the validity of the ANOVA.

The hypothesis was established as follows:

- H_0: The mean monthly precipitation is equal under different phases of the climate index.
- H_1: The mean monthly precipitation is different for at least two different phases of the climate index.

The interpretation of the ANOVA test is straightforward for PDO and AMO since they have only two levels. This is not the case for ENSO, where three levels are possible.

It is important to recall that these climate oscillations do not happen in isolation in the atmosphere. There have been proposals that these climate oscillations interact with each other. For this reason, an ANOVA considering the interaction between climate oscillations was conducted. The hypothesis for the interaction was established as follows:

- H_0: there is no interaction between climate oscillations
- H_1: there is an interaction between climate oscillations.

Finally, given that there is no evaluation of the mean precipitation between specific phases of ENSO, a Tukey's honestly significant difference (HSD) test was performed to observe if the mean precipitation is different between pairs of phases of the MEI.

2.5 Linear regression

A factorial design was performed with a number of factors k = 3, with three levels for ENSO and two levels for AMO and PDO. Hence, 12 combinations were possible. The rationale is that different combinations of the climate indices will produce different amounts of monthly precipitation. Linear regression analyses were conducted for each month and sub-basin in the watershed. Since the monthly correlations of section 2.3 were computed for the entire watershed, including all sub-basins is essential. This approach facilitates comparing it with the overall behavior of the watershed. Additionally, including all months enables the differentiation of behavior across time, considering the diverse precipitation values of the sub-basins.

It is important to note that in this study, it is assumed that ENSO, AMO, and PDO are independent to enhance the applicability of linear regression. Independence between ENSO and PDO has already been characterized (Wills et al., 2018). Our procedure is extensively discussed in Kleijnen (2015) and described next. The design matrix is defined in Eq. (7). Columns in the matrix represent the phases of ENSO, PDO, and AMO, respectively.

$$[D] = \begin{bmatrix} 1 & 1 & -1 \\ 1 & 1 & 1 \\ 1 & -1 & 1 \\ 1 & -1 & -1 \\ 0 & 1 & -1 \\ 0 & 1 & 1 \\ 0 & -1 & 1 \\ 0 & -1 & -1 \\ -1 & 1 & -1 \\ -1 & 1 & 1 \\ -1 & -1 & 1 \\ -1 & -1 & -1 \end{bmatrix} \tag{7}$$

Adding the column vector of identities to the left to compute the intercept of the regression model yields Eq. (8).

$$[X] = \begin{bmatrix} 1 & 1 & 1 & -1 \\ 1 & 1 & 1 & 1 \\ 1 & 1 & -1 & 1 \\ 1 & 1 & -1 & -1 \\ 1 & 0 & 1 & -1 \\ 1 & 0 & 1 & 1 \\ 1 & 0 & -1 & 1 \\ 1 & 0 & -1 & -1 \\ 1 & -1 & 1 & -1 \\ 1 & -1 & 1 & 1 \\ 1 & -1 & -1 & 1 \\ 1 & -1 & -1 & -1 \end{bmatrix} \tag{8}$$

Next, the inverse of the information matrix ([X]^{T}[X]) was computed:

$$\Sigma_{\hat{\beta}} = \left([X]^T[X]\right)^{-1} \leftrightarrow \left[\Sigma_{\hat{\beta}}\right] = \begin{bmatrix} 0.083 & 0 & 0 & 0 \\ 0 & 0.125 & 0 & 0 \\ 0 & 0 & 0.083 & 0 \\ 0 & 0 & 0 & 0.083 \end{bmatrix} \quad (9$$

Next, L was computed:

$$[L] = \Sigma_{\hat{\beta}}[X]^T \quad (10)$$

The response variable was computed using the average precipitation recorded in the Nazas-Aguanaval watershed during the period 1981-2021, when the conditions established in the design matrix were observed. Finally, the least squares estimator was used to compute the vector of regression parameters (Eq. [11]). Ultimately, the linear regression model is described in Eq. (12), where [y] represents the absolute precipitation anomaly (in mm), which is a deviation from the mean monthly precipitation, [$\hat{\beta}$] represents the regression coefficients, [X] the experimental matrix described in Eq. (2) and the residuals for this model.

$$\left[\hat{\beta}\right] = [L][\omega] \quad (11)$$

$$[y] = [X]\left[\hat{\beta}\right] + [e] \quad (12)$$

Finally, the absolute anomalies were computed for the months where the regression model was statistically significant (α=0.10) and the relative anomalies were computed based on mean monthly precipitation for each combination of phases of the climate indices and the mean monthly precipitation value.

3. Results and discussion

3.1 Comparison of observational and satellite data

The ANOVA for time series 1 and 2 reported no statistically significant differences between unmodified and modified mean annual precipitation datasets. There is confidence that the statistical treatment did not affect the natural variance of precipitation data. From this moment onwards, the results refer to modified time series.

Figure 2 displays annual and monthly time series comparisons between the climate and satellite data from 1981-2008. A visual inspection suggests a strong similarity in the behavior of the two data sets. To verify this mathematically, different correlation coefficients between the climate and satellite data were calculated, as shown in Table II. All correlation coefficients were found to be statistically significant at a level of 0.0001, providing further evidence of the similarity between the two data sets. These results support the use of satellite data as a reliable alternative to climate data for this period and study area, as previously found (Hernández-Romero et al., 2022).

Figure 3 shows scatter diagrams where the time series are compared. The red confidence interval encompasses the values of surface stations time series, while the blue and green confidence intervals encompass the comparison of CHIRPS time series with 28 and 46 stations, respectively. During the wet season (June-October), the closeness of these confidence intervals is higher than that of the arid season (November-May). During the latter, it is possible to observe that CHIRPS underestimate surface stations-based precipitation, which corroborates the findings of Perdigón-Morales et al. (2018). Interestingly, outliers across October to January (dry months) were found for the highest values of precipitation.

Correlations results are reported in Table II. Correlations between time series of surface stations are high; the lowest was recorded for March (r = 0.8125). Correlations between satellite and surface station data are lower, but they remain relatively high, considering the type of data being analyzed. The lowest of them was the Kendall coefficient computed for March in the correlation with time series 1, with a coefficient of 0.5791. Notably, 77% of the correlation coefficients of time series 3 with time series 2 (more stations) are higher than with time series 1 (less stations). Interestingly, the lowest correlation values for the three methods are reported during the dry period (February-May), which can be verified visually in Figure 2 because extreme values of precipitation are better described during the wet season (June, July, and September). This suggests that satellite data performed better in describing wet periods for this watershed.

We show that differences between Spearman and Pearson correlations are in the same order of magnitude

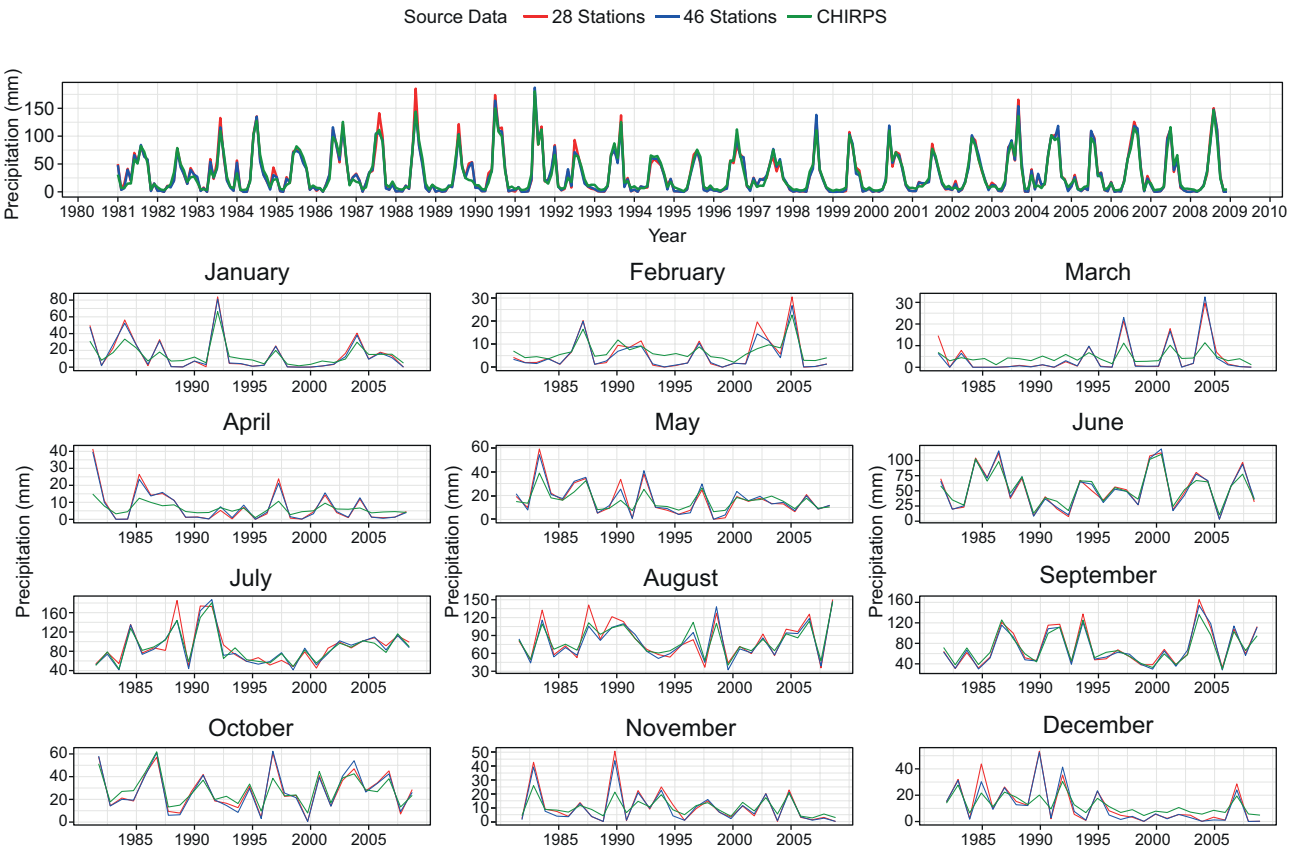

Fig. 2. Comparison between monthly precipitation time series computed using surface stations and satellite aggregated by year and disaggregated by month.

Table II. Correlations between surface stations and satellite data for monthly precipitation in the Nazas-Aguanaval watershed.

Month	Pearson correlations			Kendall correlations			Spearman correlations		
	r_1	r_2	r_3	τ_1	τ_2	τ_3	ρ_1	ρ_2	ρ_3
Full-year	0.9880	0.9478	0.9510	0.9327	0.8299	0.8410	0.9925	0.9597	0.9639
January	0.9418	0.8586	0.8653	0.9482	0.8207	0.7937	0.9869	0.9359	0.9250
February	0.9597	0.7347	0.7777	0.8927	0.5536	0.5608	0.9744	0.7538	0.7515
March	0.8125	0.7916	0.7113	0.9289	0.5738	0.6013	0.9859	0.7355	0.7615
April	0.9800	0.7895	0.7887	0.8992	0.7073	0.7338	0.9759	0.8666	0.8770
May	0.9838	0.9339	0.9370	0.9206	0.8148	0.7989	0.9852	0.9343	0.9250
June	0.9937	0.9763	0.9836	0.9524	0.8783	0.9153	0.9929	0.9748	0.9847
July	0.9378	0.9188	0.9773	0.7566	0.7407	0.8783	0.9113	0.9015	0.9726
August	0.9576	0.9413	0.9663	0.8677	0.8201	0.8571	0.9699	0.9371	0.9633
September	0.9880	0.9706	0.9756	0.8519	0.8360	0.8360	0.9655	0.9540	0.9458
October	0.9915	0.9350	0.9355	0.9471	0.8148	0.8042	0.9923	0.9398	0.9365
November	0.9769	0.8935	0.9265	0.9206	0.7831	0.8095	0.9808	0.9250	0.9414
December	0.9788	0.9420	0.9554	0.8730	0.8201	0.8413	0.9726	0.9496	0.9584

Subscript 1 stands for correlations between station data from 28 and 46 stations, while subscripts 2 and 3 stand for satellite data against 28 and 46 stations, respectively.

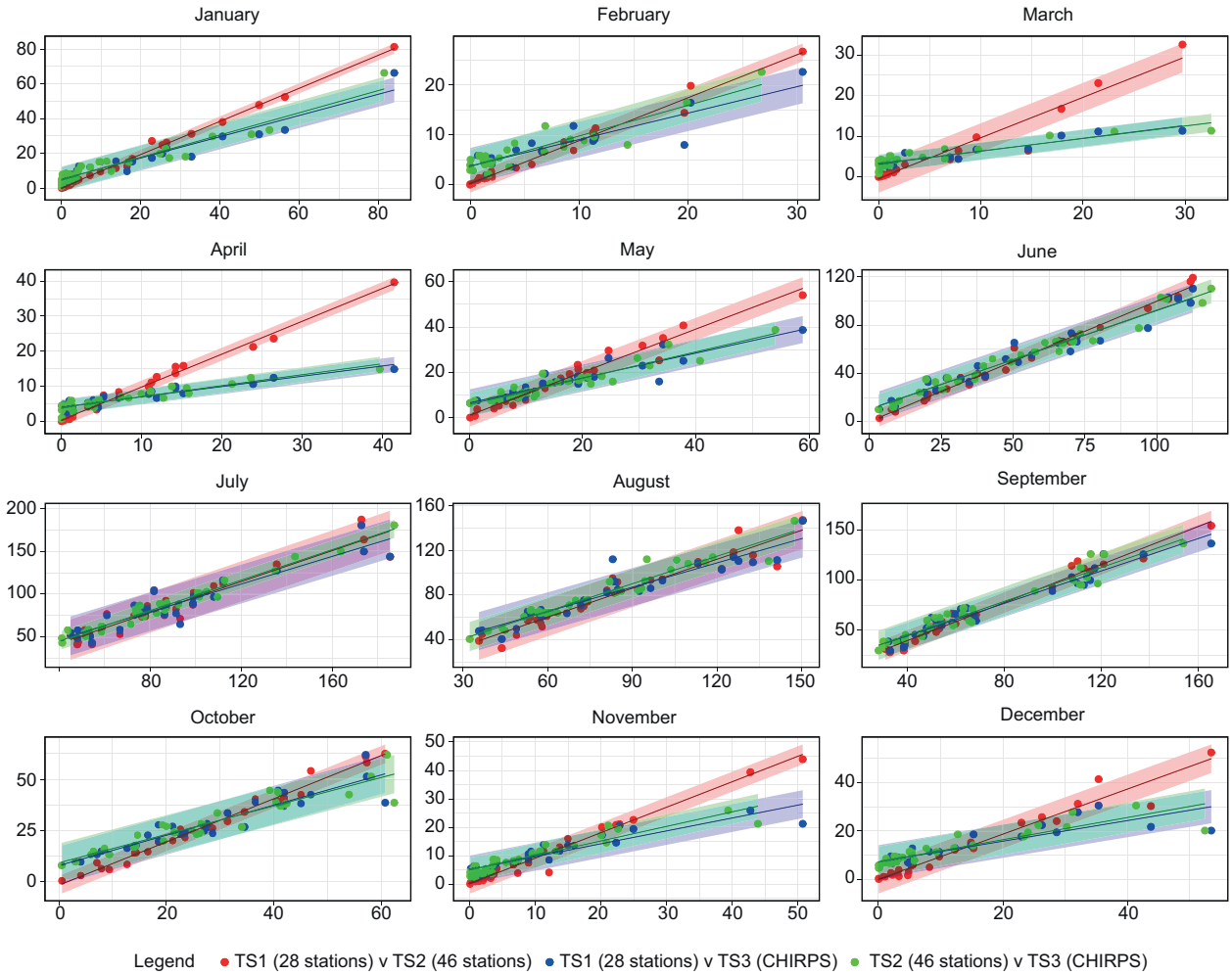

Fig. 3. Comparison between paired precipitation datasets using surface stations and satellite data disaggregated by month. The *x*- and *y*-axis indicate monthly precipitation (mm) from both data sources. The straight line indicates the linear regression line, while the shaded area shows the range that encompasses two times the standard deviation.

and support the use of satellite data. Spearman is a non-parametric method, which means that it does not rely on the data distribution. Conversely, Pearson is a parametric method supported by the normality assumption. In general, precipitation does not follow a normal distribution; hence, Box-Cox transformation is needed. Nevertheless, one of Box-Cox's requirements is that data must be non-zero and positive, which is absent in precipitation records since there can be months with no rainfall at all. In this study area, climate data reported 12 months without rainfall, which limits Box-Cox transformation unless a modification to data is made to transform from zero to one (Log(0) is undefined). In summary, the non-normal distribution of data, the physical interpretation, and the ease of computing correlations support the use of the Spearman correlation method. Another strength of the Spearman correlation method is that it is robust to outliers compared to Pearson (de Winter et al., 2016). Considering that in the future droughts will be more intense because of climate change (Martínez-Austria, 2020), this will increase precipitation data outliers.

Considering these results, it is valid to use satellite data in this study area because it offers a higher availability period (1981-2021) in comparison with station data (1979-2008). Besides, this satellite data are calibrated with data provided by the Servicio

Meteorológico Nacional (National Weather Service, SMN) (Funk et al., 2015) and have been successfully used to perform hydrologic modeling in the high plains of Mexico (Hernández-Romero et al., 2022).

3.2 Monthly precipitation teleconnections with ENSO, PDO, and AMO

In only two of the monthly datasets (June and September), there was a failure to reject the null hypothesis of the Shapiro-Wilk test. In the remaining months, the null hypothesis was rejected.

The results of teleconnections are reported in Table III and Figure 4. It is noticeable that the results are consistent between MEI, ONI, and Nino3.4. Interestingly, lower correlation values are observed during the wet season (June-September) and higher correlations are observed in the dry period (October to May). This is corroborated by Villanueva-Díaz et al. (2022), who reported that the impact of ENSO was especially noticeable during this season, which is explained by the modulation by ENSO of cold fronts that transport humidity to the Nazas-Aguanaval watershed during this season (Zermeño-Díaz and Gómez-Mendoza, 2023).

These results are supported by Cleaveland et al. (2003), who studied the same region and reported that ENSO correlation was found during the period November-March between 1894 and 1993. This period belongs to the dry season in the Nazas-Aguanaval region. The correlation of MEI with October-March precipitation is positive, which reflects that when a positive phase of ENSO is present, there is an increase in precipitation; conversely, less precipitation is expected when the phase of ENSO is negative. Besides, the intensity of the correlation varies with time, increasing gradually until reaching its peak in December, during the mature phase of ENSO, and then gradually decreasing during the first months of the year. Additionally, the same sign correlations for the period November-February were reported by Villanueva-Díaz et al. (2021), who analyzed the SOI effects on precipitation over the high plains of Mexico. In the same fashion, the same relationship was reported but for the period January-September in a region of north-eastern Mexico (Gutiérrez-García et al., 2020)

The effect of ENSO on regional annual SPI in this watershed was documented by Esquivel-Arriaga et al. (2019), who reported that the relationship between the regional annual SPI and the Niño3.4 presents a correlation coefficient of $r = 0.27$ ($p < 0.05$) In the same region, Villanueva-Díaz et al. (2022) reported that ENSO (SOI) had a Pearson correlation coefficient with precipitation in the high plains of –0.24 ($p = 0.0003$) for December-January during 1753-1977, MEI a correlation of 0.25 ($p = 0.0004$) for January-December between 1871 and 2003, and

Table III. Correlations between climate indices and monthly precipitation in the Nazas-Aguanaval watershed.

Month	Mean monthly precipitation (mm)	Spearman correlations				
		MEI	ONI	Niño 3.4	PDO	AMO
January	13.10	**0.4811**	**0.4117**	**0.4050**	**0.3837**	–0.2663
February	6.75	**0.4165**	**0.4028**	**0.4284**	0.2226	–0.0354
March	5.07	**0.4160**	**0.4303**	**0.4821**	0.2952	0.0631
April	5.58	0.1333	0.1072	–0.0051	**0.3753**	**–0.5001**
May	14.10	0.1326	**0.3815**	0.2330	0.2800	**–0.4160**
June	50.36	–0.1966	–0.1056	–0.2094	–0.0015	**–0.3620**
July	86.74	–0.1694	–0.1008	–0.1372	–0.2873	0.1421
August	78.78	–0.1449	–0.0483	–0.0374	–0.0105	0.1637
September	75.71	0.1589	0.2501	0.2492	0.1078	0.2638
October	27.73	**0.4341**	**0.4792**	**0.4528**	0.1717	–0.0461
November	9.95	**0.5347**	**0.5075**	**0.4763**	**0.5134**	**–0.3604**
December	11.72	**0.5929**	**0.5226**	**0.5193**	**0.3416**	**–0.3761**

Numbers in bold indicate statistical significance ($\alpha = 0.05$).

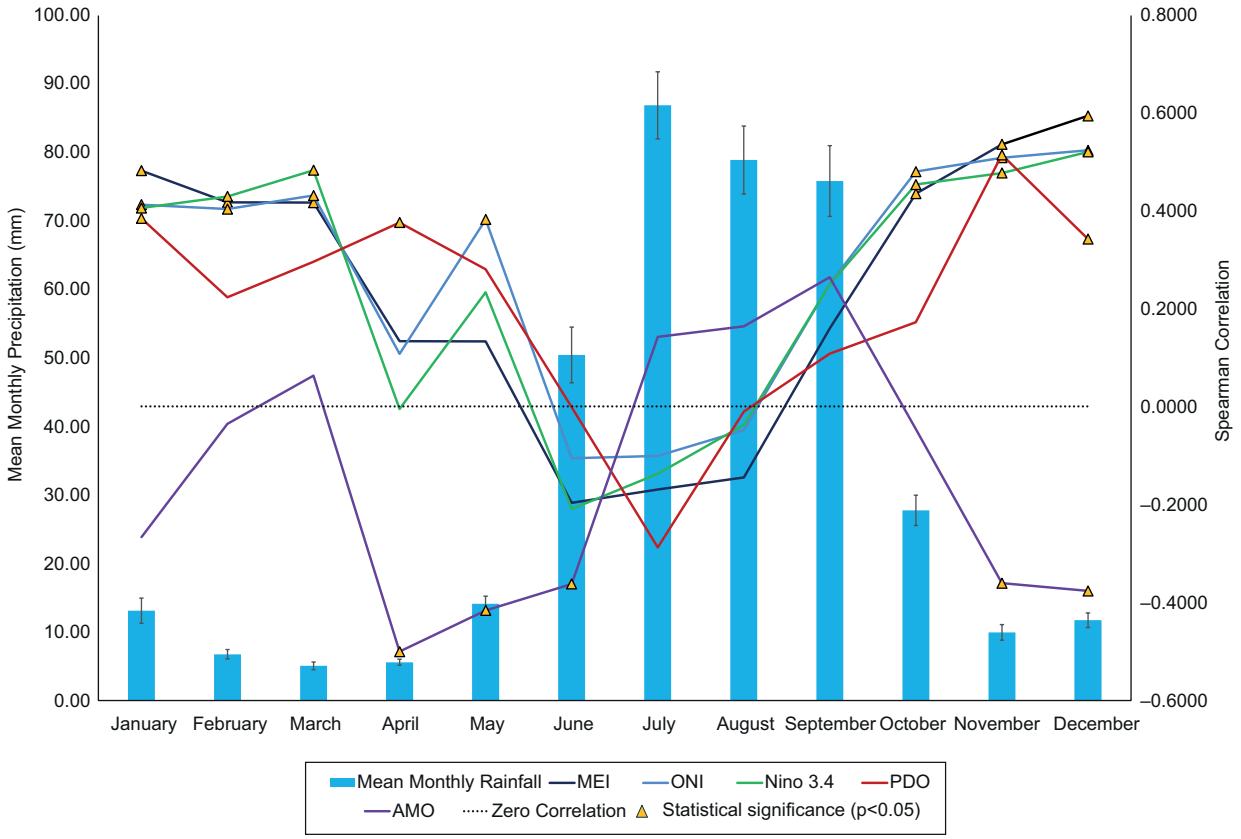

Fig. 4. Hyetograph and teleconnections observed in the Nazas-Aguanaval watershed (1981-2021).

TRI a correlation of 0.28 (p = 0.0039) during October-March in the period 1894-1995. These studies support the findings of this study, which states that ENSO influences precipitation and that its effect is stronger during winter.

As shown in Table III and Figure 4, correlations of PDO with monthly precipitation are mostly positive, and they show a temporal behavior similar to that of ENSO, although, in the former, correlations are only statistically significant for November and April. Additionally, we observed that PDO has a negative correlation during June-August, although it is not statistically significant (a = 0.05). This result is contrasted with those reported by Villanueva-Díaz et al. (2022), who found positive PDO influences for July-October in the period 1948-2003, with a Pearson correlation coefficient of 0.30 (p = 0.0250). The difference in the results can be attributed to the fact that these authors conducted their study in the Upper Nazas watershed, which is the most western sub-basin in the Nazas-Aguanaval watershed; hence, precipitation is more likely to be influenced by Pacific moisture and modulated by PDO. Additionally, they considered a much longer period of study and a different correlation method.

Figure 4 shows that PDO and ENSO correlations increase during the dry period (October-May) and decrease during the wet period. Conversely, correlations of AMO with monthly precipitation were statistically significant for April-June, November, and December but their sign is negative, meaning that during these months, a positive phase of AMO will be associated with negative precipitation anomalies and vice versa. These results are supported by Villanueva-Díaz et al. (2022), who reported that AMO influenced precipitation from October and March in the period 1857-2003 with a Pearson correlation coefficient of –0.43. AMO affects precipitation in the region because it modifies moisture advection that eventually will reach the eastern Sierra Madre, atmospheric pressure systems, and other features of atmospheric circulation.

Previously, Villanueva-Díaz et al. (2021) reported that the influence of PDO and AMO in November-February precipitation was not significant in another watershed in the Mexican high plains, while Gutiérrez-García et al. (2020) mentioned that PDO positively influenced precipitation during December-June (1970-1989) and AMO negatively influenced precipitation during April-June (1950-1969) in another watershed in northeastern Mexico. Precipitation in the Altiplano, where the Nazas-Aguanaval watershed is located, is more affected when there is a transition between El Niño and La Niña and is also modulated by the effect of PDO and AMO (Vega-Camarena et al., 2023).

Similarly, positive (negative) phases of ENSO and PDO were associated with wet (dry) periods in northern Mexico for all seasons (Mijares-Fajardo et al., 2023). However, some studies report that the effects of La Niña during spring explain less than 10% of the interannual variability in precipitation of northwestern Mexico (Zermeño-Díaz and Gómez-Mendoza, 2023). Findings from these studies exhibit divergent findings, underscoring the need for future research within this watershed and other regions across Mexico. Both isolated and coupled effects of climate oscillations must be considered in this endeavor. Furthermore, since evaluating these teleconnections is important for water resources management, performing this analysis at a watershed scale, as done in this study, is encouraged.

3.3 Monthly ANOVA

An exploratory box and whisker plot of the response of precipitation to ENSO is shown in Figure 5. For the entire watershed, we observe that there are statistically significant differences in precipitation, according

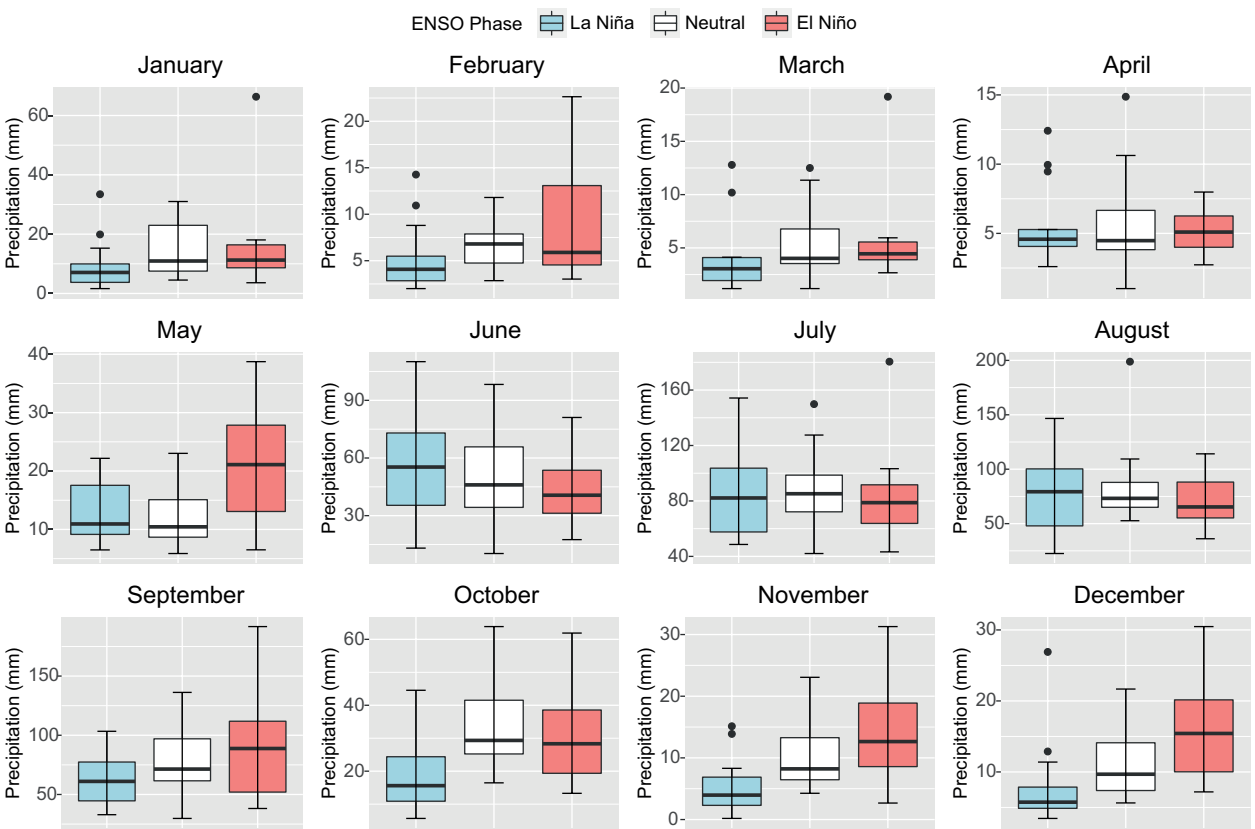

Fig. 5. Box and whisker plot for the MEI effect on monthly precipitation in the Nazas-Aguanaval watershed (1981-2021). The black center line denotes the median value (50th percentile); the black box encompasses the 25th to 75th percentiles of the dataset; whiskers indicate the 25th percentile + 1.5 times the interquartile range (IQR) and the 75th percentile +1.5 IQR, and black dots indicate the outliers.

to the MEI phase. There is a positive influence of MEI on precipitation between October and May, while between June and September, the response is reversed, and the opposite effect is observed. During the former period, a positive phase of ENSO produces more precipitation than neutral and negative phases, especially during October, December, and February. The opposite occurs during the latter period. In addition, the interquartile range of the negative phase is shorter than the neutral and El Niño phase (positive), especially during winter.

Overall, the influence of the MEI on precipitation in all sub-basins is statistically significant at the 0.05 level during certain months. The aforementioned influence of ENSO is preserved for the Upper and Lower Nazas sub-basins, although the months where it is evident are respectively November-May (positive), June-October (negative), September-May (positive), and June-October (negative) (Figs. S1-S3 in the supplementary material). This suggests that the effect of ENSO is more prolonged in the lower sub-basin. The upper Aguanaval sub-basin reports notable ENSO influence during September, while for the rest of the year, the behavior is not influenced by ENSO (Fig. S4). The lower Aguanaval sub-basin reports more influence from MEI during September-February and May, as can be seen from the results shown in Table IV and Figure S5. Besides the visualization, these results are supported by the ANOVA (Table SI).

In Figure S6, the influence of PDO in monthly precipitation in the full Nazas-Aguanaval watershed can be observed. The months of November-June show a positive relationship between precipitation and the PDO phase, following the correlations previously found. July-October exhibit marginal differences between precipitation during distinct phases of PDO. Similar behavior is observed in the Upper (Fig. S7), Middle (Fig. S8), and Lower (Fig. S9) Nazas watershed. Finally, in the Upper (Lower) Aguanaval watershed, the relationship is positive during October-June (November-May), and it is negative in the remaining months (Figs. S10 and S11). However, in contrast to ENSO, the impact of PDO is not statistically significant throughout the year, except for January, when it influences all sub-basins except the lower Aguanaval sub-basin. In the upper Aguanaval sub-basin, the impact is noticeable in November, while in both the Nazas and lower Aguanaval sub-basins, it is evident in May (Table SII).

Across the Nazas-Aguanaval watershed, AMO has a negative relationship with precipitation during most of the year. This means that a positive (negative) phase of AMO is associated with a drier (wetter) condition, except during summer when there is a shift in this relationship (Figs. S12-S17). However, this influence is statistically significant only between April and May for the Middle Nazas and the Aguanaval sub-basins and for April for Upper and Lower

Table IV. ANOVA p-values of precipitation under the influence of MEI.

Month	Full basin	Upper Nazas	Middle Nazas	Lower Nazas	Upper Aguanaval	Lower Aguanaval
January	**0.0308**	**0.0481**	0.0557	**0.0173**	0.0573	**0.0188**
February	**0.0141**	**0.0232**	**0.0160**	**0.0113**	**0.0247**	**0.0123**
March	0.0506	0.0548	**0.0482**	**0.0498**	0.2030	0.0661
April	0.8371	0.9601	0.8639	0.7033	0.8807	0.8025
May	0.1236	0.4734	0.2900	**0.0218**	0.3301	**0.0131**
June	0.3150	0.1847	0.6435	0.5265	0.3695	0.8943
July	0.8589	0.8703	0.8742	0.6884	0.8468	0.5574
August	0.9607	0.7593	0.6633	0.9439	0.6066	0.8746
September	0.1054	0.2057	0.1121	**0.0459**	0.2128	**0.0210**
October	**0.0183**	0.1895	**0.0246**	**0.0116**	**0.0014**	**0.0027**
November	**0.0001**	**0.0006**	**0.0000**	**0.0002**	**0.0003**	**0.0009**
December	**0.0002**	**0.0002**	**0.0005**	**0.0004**	**0.0013**	**0.0002**

Numbers in bold indicate statistical significance ($\alpha = 0.05$).

Nazas. In addition, there is statistically significant effects in December on the Upper and Middle Nazas watersheds (Table SIII).

The combined effect of the climate indices was evaluated using ANOVA. Interactions between combinations of MEI with PDO and AMO register practically the same effects as MEI alone, meaning that ENSO drives the effects on precipitation. Additionally, the interaction of PDO with AMO reports scarce statistically significant results. This is a first approximation for observing the interaction of different climate indices, as suggested previously in the literature (Mijares-Fajardo et al., 2023; Vega-Camarena et al., 2023).

3.4 Linear regression

The linear regression model describes the absolute anomaly based on the combinations of phases of the three climate indices. The determination coefficients are reported in Table V. These combinations, defined in Eq. (7), indicate different phases of the climate oscillation. With three climate indices considered (ENSO, PDO, and AMO), where ENSO has three phases (positive, neutral, and negative) and PDO and AMO have two phases each (positive and negative), there are 12 possible combinations of these phases. By considering this, it becomes possible to compute the expected absolute anomalies for the months where statistically significant results were found. Moreover, relative anomalies with respect to mean monthly precipitation can also be calculated. It is important to note that not all combinations of the phases of the climate oscillations have been observed during the studied period. This is shown in the empty cells of Tables VI and VII.

The results from Tables VI and VII can be used to estimate monthly precipitation anomalies, depending on the current phase of climate indices. These tables express the extent to which rainfall deviates from the mean value within a specific month for a given sub-basin, indicating either increases or decreases in precipitation.

In that sense, Table VI illustrates that, for the entire Nazas-Aguanaval watershed, when ENSO is in a negative phase (La Niña), we observe negative anomalies in 70% of the statistically significant monthly records and conversely, we observe positive anomalies in 70% of cases when ENSO is in a positive phase. This means that La Niña (El Niño) favors dry (wet) months in the Nazas-Aguanaval watershed during January, February, April, September and December. When ENSO is in the neutral phase, 40% of anomalies are positive associated to wet months, 45% are negative associated to dry months, and the remaining 15% is from combinations that have not been observed. Dry months are especially predominant when both ENSO and PDO are in a negative phase and their magnitude is superior during January. Likewise, dry months are more frequent when both

Table V. Linear model determination coefficients for different months and sub-basins in the Nazas-Aguanaval.

Month	Full basin	Upper Nazas	Middle Nazas	Lower Nazas	Upper Aguanaval	Lower Aguanaval
January	**0.6300**	**0.7422**	**0.6182**	**0.6063**	0.3406	0.5008
February	**0.7635**	**0.7379**	**0.6728**	**0.8192**	**0.6574**	**0.7321**
March	0.1544	0.1280	0.2629	0.3603	0.2535	0.2300
April	**0.6760**	**0.6901**	**0.8491**	0.2830	**0.7519**	0.2875
May	0.2009	0.0740	0.1888	0.1879	0.3949	0.4156
June	0.2417	0.2911	0.2602	0.2938	0.1297	0.1360
July	0.3608	0.1769	0.3210	0.3934	0.4314	0.5596
August	0.0763	0.0540	0.0075	0.2665	0.1365	0.2190
September	**0.6684**	0.4140	0.6139	0.5304	**0.6673**	0.5957
October	0.4628	0.2457	0.3796	0.3760	**0.6237**	0.5114
November	0.4395	**0.6963**	**0.6343**	0.4304	0.5056	0.3687
December	**0.7884**	**0.6708**	**0.7008**	**0.6119**	**0.7383**	**0.5814**

Numbers in bold indicate statistical significance ($\alpha = 0.05$).

Table VI. Monthly precipitation anomalies associated with changes in the phase of climate oscillations in the Nazas-Aguanaval and Aguanaval watersheds.

ENSO phase	PDO phase	AMO phase	Nazas-Aguanaval full watershed					Upper Aguanaval					Lower Aguanaval	
			January	February	April	September	December	February	April	September	October	December	February	December
Positive	Positive	Negative	–36.4%	27.0%	–14.8%	–4.2%	7.9%	53.7%	–23.3%	4.3%	28.3%	12.0%	29.2%	12.3%
Positive	Positive	Positive	17.8%	90.2%	1.2%	55.2%	17.0%	139.7%	–37.1%	65.3%	47.2%	22.9%	102.7%	30.6%
Positive	Negative	Positive	107.9%	27.3%	4.3%	6.0%	49.5%	23.4%	20.2%	–14.7%	12.7%	43.1%	35.3%	41.0%
Positive	Negative	Negative	–19.6%			17.4%	105.4%			19.3%	16.4%	73.8%		117.2%
Neutral	Positive	Negative			–22.2%	26.7%	–21.6%		–17.5%	8.7%	18.2%	–32.8%		–17.7%
Neutral	Positive	Positive	13.1%	–11.7%	–19.2%	1.1%	–20.6%	–21.1%	–21.0%	2.3%	1.6%	–5.9%	–12.3%	–7.1%
Neutral	Negative	Positive	38.5%	–2.7%	50.0%	–18.2%	2.9%	–11.3%	64.8%	–16.1%	33.3%	9.0%	–6.8%	–10.5%
Neutral	Negative	Negative	–36.4%	10.7%	–6.7%		8.9%	–0.9%	–6.1%		18.7%	–2.3%	2.0%	1.3%
Negative	Positive	Negative	–14.7%	–56.2%		–17.4%	–2.8%	–73.8%		–30.0%	–65.6%	–10.5%	–78.1%	8.2%
Negative	Positive	Positive	–75.2%	–19.3%	–28.3%	–13.8%	–33.4%	–8.1%	–33.5%	–5.0%	–38.5%	–31.1%	–23.4%	–34.3%
Negative	Negative	Positive	23.4%	–16.7%	36.4%			–20.3%	44.5%				–15.0%	
Negative	Negative	Negative	–45.7%	–25.7%	35.8%	–31.7%	–29.4%	–33.3%	24.1%	–41.3%	–5.7%	–26.6%	–24.7%	–35.7%

Table VII. Monthly precipitation anomalies associated with changes in the phase of climate oscillations in the Nazas watershed.

ENSO phase	PDO phase	AMO phase	Upper Nazas					Middle Nazas					Lower Nazas		
			January	February	April	November	December	January	February	April	November	December	January	February	December
Positive	Positive	Negative	–46.2%	20.5%	–14.0%	31.2%	26.4%	–41.9%	18.1%	–19.3%	35.4%	–8.1%	–13.5%	10.2%	–13.2%
Positive	Positive	Positive	25.1%	59.0%	–17.4%	81.3%	10.8%	–6.1%	98.3%	–22.6%	58.1%	1.5%	40.3%	60.3%	21.8%
Positive	Negative	Positive	101.2%	21.3%	25.0%	23.2%	49.6%	116.9%	23.2%	25.3%	40.4%	63.0%	80.5%	34.6%	51.6%
Positive	Negative	Negative	–23.7%			82.9%	116.2%	–29.4%			68.8%	128.6%	–21.2%		97.6%
Neutral	Positive	Negative			–24.0%	46.2%	–28.3%			–26.7%	107.4%	–30.3%			1.4%
Neutral	Positive	Positive	14.7%	–2.3%	–21.5%	1.1%	–35.7%	12.3%	–17.6%	–19.6%	–6.1%	–30.6%	3.2%	–8.7%	–15.5%
Neutral	Negative	Positive	57.7%	–3.7%	58.3%	–19.7%	2.4%	48.8%	9.1%	49.2%	–25.9%	12.7%	34.3%	3.6%	–0.2%
Neutral	Negative	Negative	–37.5%	31.4%	–17.0%	9.6%	22.8%	–38.8%	6.6%	4.0%	25.7%	11.3%	–25.2%	8.1%	3.6%
Negative	Positive	Negative	–42.2%	–40.9%		–24.6%	16.5%	–26.5%	–37.8%		–8.0%	–27.9%	–18.4%	–49.5%	–11.8%
Negative	Positive	Positive	–78.1%	–24.9%	–37.2%	–70.2%	–41.1%	–76.3%	–9.2%	–30.1%	–73.5%	–30.1%	–71.7%	–27.4%	–26.5%
Negative	Negative	Positive	43.1%	–8.0%	67.5%	–1.2%		31.1%	–19.5%	61.5%	–15.0%		19.2%	–22.9%	
Negative	Negative	Negative	–59.2%	–28.7%	30.9%	–37.8%	–24.4%	–50.4%	–31.4%	26.8%	–48.3%	–28.9%	–33.7%	–11.8%	–35.4%

ENSO and PDO are in the positive phase, as reported in previous studies (Pavia et al., 2006; Durán-Quesada et al., 2020; Gutiérrez-Garcia et al., 2020) but only during a negative phase of AMO.

When observing the anomalies disaggregated by sub-basin in the Nazas watershed (Table VII), the results are similar: 650% of the anomalies are positive during the occurrence of El Niño and 75% are negative during the occurrence of La Niña. Similarly, in the Aguanaval watershed (Table VI), 79% of the anomalies are positive when El Niño is present and 71% are negative when La Niña is present. This means that El Niño (La Niña) favors wet (dry) months across this watershed.

Across the entire watershed, the quartiles of anomalies were –19.89%, –2.73%, and 19.18% with a minimum and maximum of –75.25% and 107.93%, respectively, as shown in Table VI. In addition, negative anomalies are slightly more frequent, as indicated by the 50 percentiles. This holds true across all sub-basins, with the highest 50 percentile achieved at –7.05% in the Middle Nazas. The Upper Aguanaval shows the maximum relative anomaly at 139.75% for February, which happened in a circumstance of positive phases for all indices. Conversely, the Upper Nazas and Lower Aguanaval show the minimum relative anomaly at –78.08% for January and February, respectively.

4. Conclusions

Observational data was recovered, and filling techniques were used for estimating missing observational precipitation values. Two observational time series derived from surface station data were compared with a satellite-derived time series. The statistical analysis showed no significant differences between modified and unmodified precipitation data, indicating that the statistical treatment, based on the normal ratio method, did not affect the natural variance of the data. This illustrates the usefulness of techniques for completing non-continuous precipitation data sets. Besides, the correlation analysis of climate and satellite data revealed a strong similarity between the two datasets, with all correlation coefficients being significant. This supports the use of satellite data as a reliable source of climate data for the region from 1981 to 2008. The use of satellite data is also supported by its higher availability period and successful applications in hydrologic modeling in the study area. Finally, the need for continued efforts to improve the accuracy and availability of precipitation data, particularly in regions where data is scarce or unreliable, is demonstrated.

In addition, this study used satellite data to analyze teleconnections of monthly precipitation in the Nazas-Aguanaval watershed with three climate oscillations (ENSO, PDO, and AMO), applying Spearman, Pearson, and Kendall correlations and using three climate indices for ENSO (MEI, ONI, and Niño 3.4). It is important to note that all correlation methods yielded similar results. However, due to its robustness to outliers, ability to handle non-normally distributed precipitation data, and greater computation readiness, the Spearman method is preferred. Similarly, ONI, MEI, and Niño 3.4 showed correlations with monthly precipitation. ENSO was proven to be the oscillation that most influences precipitation in the study region given that the correlations of all three of its indices are statistically significant during the dry period (October-March), while PDO seconds in influence because it had high correlations during November-January and April. Finally, AMO showed important correlations with precipitation during April-June, November, and December but no clear association with the rainfall hyetograph was identified.

These results were verified using ANOVA. The analysis showed that the influence of MEI on precipitation is significant from October to March, with a positive impact during October to May and a reversed trend during June to September, confirming previous studies. The influence of PDO is not statistically significant throughout the year, except in January. AMO has an impact between April and May, and in December. There are also interactions between combinations of MEI with PDO and AMO that register the same effects as MEI alone, meaning that further analysis is needed to conclude if the influence of PDO and AMO modifies the effects of ENSO in the study region.

The results from the linear regression model indicate that the estimation of monthly precipitation is not consistent across all months. While the model performs well for December-February, September and April (Nazas-Aguanaval watershed), its accuracy falls short for others. However, for Upper and Middle

Nazas, this linear regression model allows to estimate monthly precipitation anomalies for five months (November to February and April), while for the Upper Aguanaval, allowable estimations were done for February, April, September, October, and December, considering that, spatially, 97% of the runoff in the entire watershed occurs in these three sub-basins. However, from the perspective of time, the runoff does not occur during these months, because 90% of the runoff happens between July and October.

In short, the findings of this study suggest a shift in the behavior of teleconnections with ENSO during the winter season. Between October and March, a positive (negative) phase of ENSO will produce wet (dry) months in this season. During the remaining months, a positive (negative) phase of ENSO will produce dry (wet) months, although not with statistical significance.

The contribution to hydrologic and climate research is demonstrated by showing that satellite data is useful for analyzing the influence of climate oscillations on precipitation and proving that ANOVA is an effective methodology for these analyses. Additionally, we proposed a method for computing absolute precipitation anomalies based on the phases of different climate oscillations. These findings are valuable for readily informing decision-makers about these phenomena' impacts and developing more effective water management strategies, including dam operation policies, groundwater management, and the deployment of emergent efficiency actions. Finally, the approach proposed in this manuscript can be replicated in watersheds lacking surface stations, where data is insufficient or unreliable. This enables countries exposed to these climate oscillations to conduct their studies.

One limitation of this research is that it categorizes the phases of climate oscillations into two or three levels, rather than using real continuous data. Further research should examine what would happen in a regression model considering continuous monthly climate indices measurements. Moreover, the results of this study underscore the importance of studying the influence of climate oscillations in arid and semiarid watersheds across the world. Additionally, this analysis considered temporal on-phase correlations; however, studying the correlations out of phase can provide more insights into the lagged influence of climate oscillations on precipitation. Next, interactions were left outside the linear regression model, which may be of interest, as reported by the ANOVA. Finally, this study considers the effects of ENSO, AMO, and PDO; further research might explore other climate oscillations.

Acknowledgments

This research was funded by the Consejo Nacional de Humanidades, Ciencia y Tecnología (CONAHCyT) with a National Graduate Scholarship and the Universidad de las Américas Puebla with an Academic UDLAP Research Scholarship. The authors would like to thank both institutions. The first author would like to thank professors Jose M. Cabrera, Claudia Calvario, and Daniela Cortés, from UDLAP, for their feedback on this work.

References

Álvarez-Olguín G, Escalante-Sandoval C. 2017. Modes of variability of annual and seasonal rainfall in Mexico. Journal of the American Water Resources Association 53: 144-157. https://doi.org/10.1111/1752-1688.12488

Bhattacharya T, Chiang JCH. 2014. Spatial variability and mechanisms underlying El Niño-induced droughts in Mexico. Climate Dynamics 43: 3309-3326. https://doi.org/10.1007/s00382-014-2106-8

Blanca MJ, Alarcón R, Arnau J, Bono R, Bendayan R. 2017. Non-normal data: Is ANOVA still a valid option? Psicothema 29: 552-557. https://doi.org/10.7334/psicothema2016.383

Bravo JL, Azpra E, Zarraluqui V, Gay C. 2014. Some variations of the rainfall in Mexico City from 1954 to 1988 and their statistical significance. Atmósfera 27: 367-376. https://doi.org/10.1016/S0187-6236(14)70035-9

Cleaveland MK, Stahle DW, Therrell MD, Villanueva-Díaz J, Burns BT. 2003. Tree-ring reconstructed winter precipitation and tropical teleconnections in Durango, Mexico. Climatic Change 59: 369-388. https://doi.org/10.1023/A:1024835630188

CONABIO. 2001. Estaciones climatológicas (ERIC): catálogo de metadatos geográficos. Comisión Nacional para el Conocimiento y Uso de la Biodiversidad. Available at: http://geoportal.conabio.gob.mx/metadatos/doc/html/estclimgw.html#_stdorder (accessed 2024 June 26)

De Winter JCF, Gosling SD, Potter J. 2016. Comparing the Pearson and Spearman correlation coefficients across distributions and sample sizes: A tutorial using simulations and empirical data. Psychological Methods 21: 273-290. https://doi.org/10.1037/met0000079

Durán-Quesada AM, Sorí R, Ordóñez P, Gimeno L. 2020. Climate perspectives in the Intra-Americas seas. Atmosphere 11: 959. https://doi.org/10.3390/atmos11090959

Enfield DB, Mestas-Núñez AM, Trimble PJ. 2001. The Atlantic Multidecadal Oscillation and its relation to rainfall and river flows in the continental U.S. Geophysical Research Letters 28: 2077-2080. https://doi.org/10.1029/2000GL012745

Esquivel-Arriaga G, Cerano-Paredes J, Sánchez-Cohen I, Velásquez-Valle MA, Flores-López F, Bueno-Hurtado P. 2019. Análisis temporal de sequías (1922-2016) en la cuenca alta del río Nazas usando el SPI y su relación con ENSO (Temporal analysis of droughts [1922-2016] in the upper Nazas River Basin using SPI and its relationship with ENSO). Tecnología y Ciencias del Agua 10: 126-153. https://doi.org/10.24850/j-tyca-2019-05-05

Funk C, Peterson P, Landsfeld M, Pedreros D, Verdin J, Shukla S, Husak G, Rowland J, Harrison L, Hoell A, Michaelsen J. 2015. The climate hazards infrared precipitation with stations – A new environmental record for monitoring extremes. Scientific Data 2: 150066. https://doi.org/10.1038/sdata.2015.66

González-Ortigoza S, Hernández-Espriú A, Arciniega-Esparza S. 2023. Regional modeling of groundwater recharge in the Basin of Mexico: New insights from satellite observations and global data sources. Hydrogeology Journal 31: 1971-1990. https://doi.org/10.1007/s10040-023-02667-w

Guevara-Polo DE, Mijares-Fajardo R. 2021. El Niño Oscilación del Sur y sus efectos sobre la precipitación en México. Entorno UDLAP 15: 26-35.

Gutiérrez-García G, Leavitt SW, Trouet V, Carriquiry JD. 2020. Tree ring-based historic hydroclimatic variability of the Baja California Peninsula. Journal of Geophysical Research: Atmospheres 125: e2020JD032675. https://doi.org/10.1029/2020JD032675

Hernández-Romero P, Patiño-Gómez C, Martínez-Austria PF, Corona-Vásquez B. 2022. Rainfall/runoff hydrological modeling using satellite precipitation information. Water Practice and Technology 17: 1082-1098. https://doi.org/10.2166/wpt.2022.048

Kleijnen JPC. 2015. Design and analysis of simulation experiments. Springer, Cham. https://doi.org/10.1007/978-3-319-18087-8

Levizzani V, Cattani E. 2019. Satellite remote sensing of precipitation and the terrestrial water cycle in a changing climate. Remote Sensing 11: 2301. https://doi.org/10.3390/rs11192301

Llanes-Cárdenas O, Norzagaray-Campos M, Gaxiola A, González González GE. 2020. Regional precipitation teleconnected with PDO-AMO-ENSO in northern Mexico. Theoretical and Applied Climatology 140: 667-681. https://doi.org/10.1007/s00704-019-03003-7

MacDonald GM, Case RA. 2005. Variations in the Pacific Decadal Oscillation over the past millennium. Geophysical Research Letters 32: L08703. https://doi.org/10.1029/2005GL022478

Magaña VO, Vázquez JL, Pérez JL, Pérez JB. 2003. Impact of El Niño on precipitation in Mexico. Geofísica Internacional 42: 313-330. https://doi.org/10.22201/igeof.00167169p.2003.42.3.949

Mantua NJ, Hare SR, Zhang Y, Wallace JM, Francis RC. 1997. A Pacific Interdecadal Climate Oscillation with impacts on salmon production. Bulletin of the American Meteorological Society 78: 1069-1080. https://doi.org/10.1175/1520-0477(1997)078%3C1069:APICOW%3E2.0.CO;2

Martínez-Austria PF. 2020. Climate change and water resources in Mexico. In: Water resources of Mexico (Raynal-Villaseñor JA, Ed.). World Water Resources, v. 6. Springer, Cham, 157-175. https://doi.org/10.1007/978-3-030-40686-8_9

McCabe GJ, Palecki MA, Betancourt JL. 2004. Pacific and Atlantic Ocean influences on multidecadal drought frequency in the United States. Proceedings of the National Academy of Sciences 101: 4136-4141. https://doi.org/10.1073/pnas.0306738101

Méndez M, Magaña V. 2010. Regional aspects of prolonged meteorological droughts over Mexico and Central America. Journal of Climate 23: 1175-1188. https://doi.org/10.1175/2009JCLI3080.1

Mijares-Fajardo R, Lobato-Sánchez R, Patiño-Gómez C, Guevara-Polo DE. 2023. Atlantic and Pacific sea surface temperature correlations with precipitation over northern Mexico. Atmósfera 38: 217-234. https://doi.org/10.20937/ATM.53257

Montero-Martínez MJ, Santana-Sepúlveda JS, Pérez-Ortiz NI, Pita-Díaz Ó, Castillo-Liñan S. 2018. Comparing climate change indices between a northern (arid) and

a southern (humid) basin in Mexico during the last decades. Advances in Science and Research 15: 231-237. https://doi.org/10.5194/asr-15-231-2018

Montero-Martínez MJ, Pita-Díaz O, Andrade-Velázquez M. 2022. Potential influence of the Atlantic Multidecadal Oscillation in the recent climate of a small basin in Central Mexico. Atmosphere 13: 339. https://doi.org/10.3390/atmos13020339

Muluken LE. 2020. Techniques of filling missing values of daily and monthly rain fall data: A review. SF Journal of Environmental and Earth Science 3: 1036.

Nadiatul Adilah AAG, Hannani H. 2021. Comparison of methods to estimate missing rainfall data for short term period at UMP Gambang. IOP Conference series: Earth and Environmental Science 682: 012027. https://doi.org/10.1088/1755-1315/682/1/012027

Nigam S, Baxter S. 2015. General circulation of the atmosphere. Teleconnections. In: Encyclopedia of atmospheric sciences (North GR, Pyle J, Zhang F, Eds.). Elsevier, 90-109. https://doi.org/10.1016/B978-0-12-382225-3.00400-X

NOAA. 2024a. Cold & Warm Episodes by Season. ONI. Climate Prediction Center, NOAA. Available at: https://origin.cpc.ncep.noaa.gov/products/analysis_monitoring/ensostuff/ONI_v5.php (accessed 2024 June 26)

NOAA. 2024b. Climate timeseries. AMO (Atlantic Multidecadal Oscillation) Index. Physical Sciences Laboratory, NOAA. Available at: https://psl.noaa.gov/data/timeseries/AMO/ (accessed 2024 June 26)

NOAA. 2024c. Multivariate ENSO Index version 2 (MEI.v2). Physical Sciences Laboratory, NOAA. Available at: https://psl.noaa.gov/enso/mei/ (accessed 2024 June 26)

NOAA. 2024d. Download Climate Timeseries: Niño 3.4 SST Index. Physical Sciences Laboratory, NOAA.. Available at: https://psl.noaa.gov/gcos_wgsp/Timeseries/Nino34/index.html (accessed 2024 June 26)

NOAA. 2024e. Pacific Decadal Oscillation (PDO). National Centers of Environmental Information, NOAA. Available at: https://www.ncei.noaa.gov/access/monitoring/pdo/ (accessed 2024 June 26)

Norzagaray-Campos M, Muñoz-Sevilla P, Espinosa-Carreón L, Ruiz-Guerrero R, González-Ocampo H, Llanes-Cárdenas O. 2016. Erosivity indicators based on rainfall in northwestern Mexico. Journal of Environmental Engineering and Landscape Management 24: 133-142. https://doi.org/10.3846/16486897.2015.1106405

Park J, Byrne R, Böhnel H. 2017. The combined influence of Pacific Decadal Oscillation and Atlantic Multidecadal Oscillation on Central Mexico since the early 1600s. Earth and Planetary Science Letters 464: 1-9. https://doi.org/10.1016/j.epsl.2017.02.013

Pavia EG, Graef F, Reyes J. 2006. PDO-ENSO effects in the Climate of Mexico. Journal of Climate 19: 6433-6438. https://doi.org/10.1175/JCLI4045.1

Perdigón-Morales J, Romero-Centeno R, Ordóñez Pérez P, Barrett BS. 2018. The midsummer drought in Mexico: Perspectives on duration and intensity from the CHIRPS precipitation database. International Journal of Climatology 38: 2174-2186. https://doi.org/10.1002/joc.5322

Perdigón-Morales J, Romero-Centeno R, Barrett BS, Ordóñez P. 2019. Intraseasonal variability of summer precipitation in Mexico: MJO influence on the Midsummer Drought. Journal of Climate 32: 2313-2327. https://doi.org/10.1175/JCLI-D-18-0425.1

Ramírez Barraza BA, González Estrada A, Valdivia Alcalá R, Salas González JM, García Salazar JA. 2019. Efficient rates for water for agricultural use in the Comarca Lagunera. Revista Mexicana de Ciencias Agrícolas 10: 539-550. https://doi.org/10.29312/remexca.v10i3.1295

Rincón-Ávalos P, Khouakhi A, Mendoza-Cano O, López-de La Cruz J, Paredes-Bonilla KM. 2022. Evaluation of satellite precipitation products over Mexico using Google Earth Engine. Journal of Hydroinformatics 24: 711-729. https://doi.org/10.2166/hydro.2022.122

Sánchez Cohen I, Inzunza Ibarra MA, Esquivel Arriaga G, Cerano Paredes J, Velásquez Valle MA, Bueno Hurtado P, Ojeda Bustamante W. 2018. The impact of climatic patterns on runoff and irrigation water allocation in an arid watershed of northern Mexico. Meteorology Hydrology and Water Management 6: 59-66. https://doi.org/10.26491/mhwm/90843

Sánchez Santillán N, Garduño López R, Vidal Zepeda R, Sánchez Trejo R. 2012. Climate change in NE Mexico: Influence of the North Atlantic Oscillation. Investigaciones Geográficas 78: 7-18.

SG. 2024. ClimateSERV 2.0. Servir Global. Available at: https://climateserv.servirglobal.net/ (accessed 2024 June 26)

Silva-Aguilera RA, Escolero O, Alcocer J, Correa Metrio A, Vilaclara G, Lozano García S. 2024. Long-term

responses of maar lakes water level to climate and groundwater variability in Central Mexico. Journal of South American Earth Sciences 139: 104861. https://doi.org/10.1016/j.jsames.2024.104861

Torres VM. 2024. A hot Spring for Mexico in 2024. Atmósfera Opinión. https://doi.org/10.20937/ATM.53377

Van Viet L. 2021. Development of a new ENSO index to assess the effects of ENSO on temperature over southern Vietnam. Theoretical and Applied Climatology 144: 1119-1129. https://doi.org/10.1007/s00704-021-03591-3

Vega-Camarena JP, Brito-Castillo L, Pineda-Martínez LF, Farfán LM. 2023. ENSO impact on summer precipitation and moisture fluxes over the Mexican Altiplano. Journal of Marine Science and Engineering 11: 1083. https://doi.org/10.3390/jmse11051083

Villanueva-Díaz J, Martínez-Sifuentes AR, Reyes-Camarillo FdR, Estrada-Ávalos J. 2021. Reconstruction of precipitation and temperature with annual growth rings of the cypress *Taxodium mucronatum* (Taxodiaceae) in Coahuila, Mexico. Revista de Biología Tropical 69: 302-316. https://doi.org/10.15517/rbt.v69i1.43249

Villanueva-Díaz J, Estrada-Ávalos J, Martínez-Sifuentes AR, Correa-Díaz A, Meko DM, Castruita-Esparza LU, Cerano-Paredes J. 2022. Historic variability of the water inflow to the Lazaro Cardenas dam and water allocation in the Irrigation District 017, Comarca Lagunera, Mexico. Forests 13: 2057. https://doi.org/10.3390/f13122057

Villate García E, Morales Hernández JC, Romo Aguilar ML, García Concepción FO, Castillo Aja R. 2023. Potential of the CHIRPS database for extreme precipitation risk studies. Assessment in the State of Jalisco (Mexico). International Journal of Sustainable Development and Planning 18: 847-855. https://doi.org/10.18280/ijsdp.180320

Wills RC, Schneider T, Wallace JM, Battisti DS, Hartmann DL. 2018. Disentangling global warming, multidecadal variability, and El Niño in Pacific temperatures. Geophysical Research Letters 45: 2487-2496. https://doi.org/10.1002/2017GL076327

Zermeño-Díaz DM, Gómez-Mendoza L. 2023. The influence of ENSO during spring over northwestern Mexico. International Journal of Climatology 43: 6420-6433. https://doi.org/10.1002/joc.8212

Supplementary Material

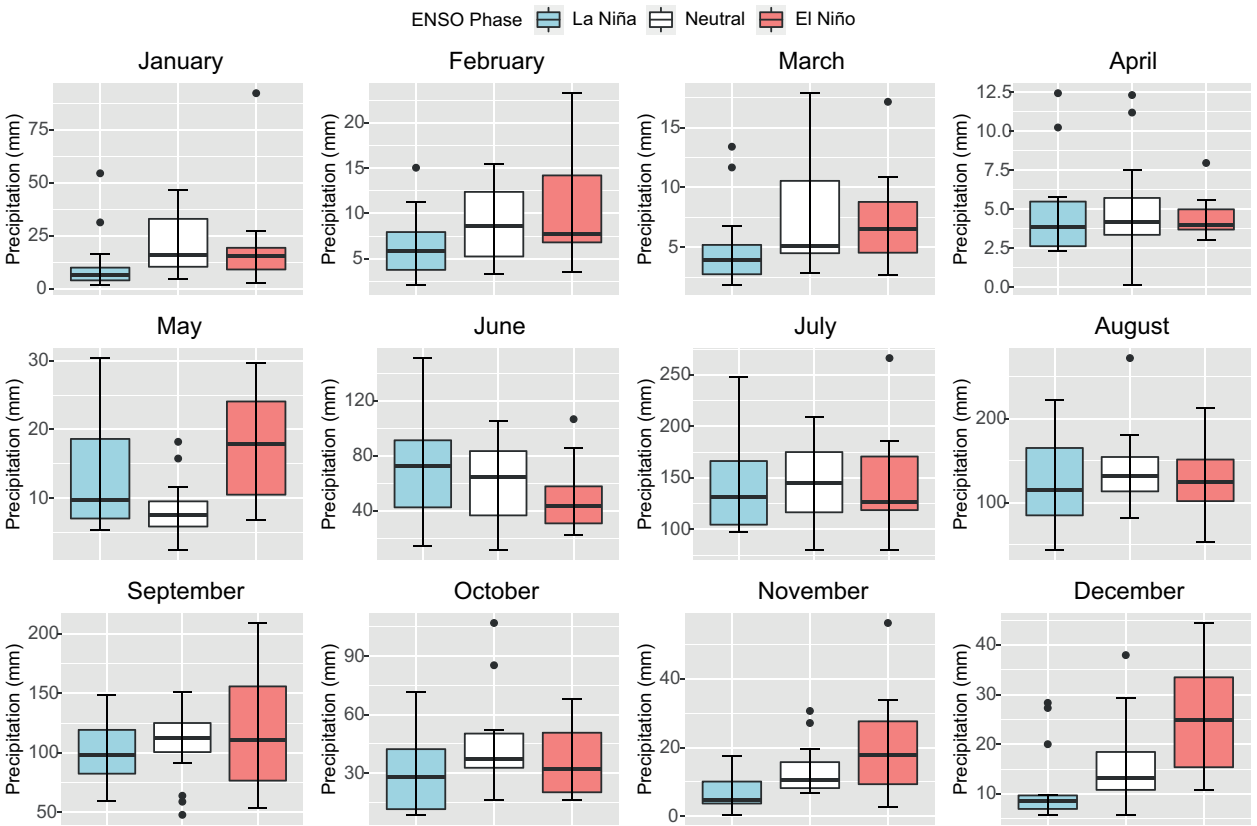

Fig. S1. Box and whisker plot for the MEI effect on monthly precipitation in the Upper Nazas watershed (1981-2021). The black center line denotes the median value (50th percentile); the black box encompasses the 25th to 75th percentiles of the dataset; whiskers indicate the 25th percentile + 1.5 times the interquartile range (IQR) and the 75th percentile +1.5 IQR, and black dots indicate the outliers.

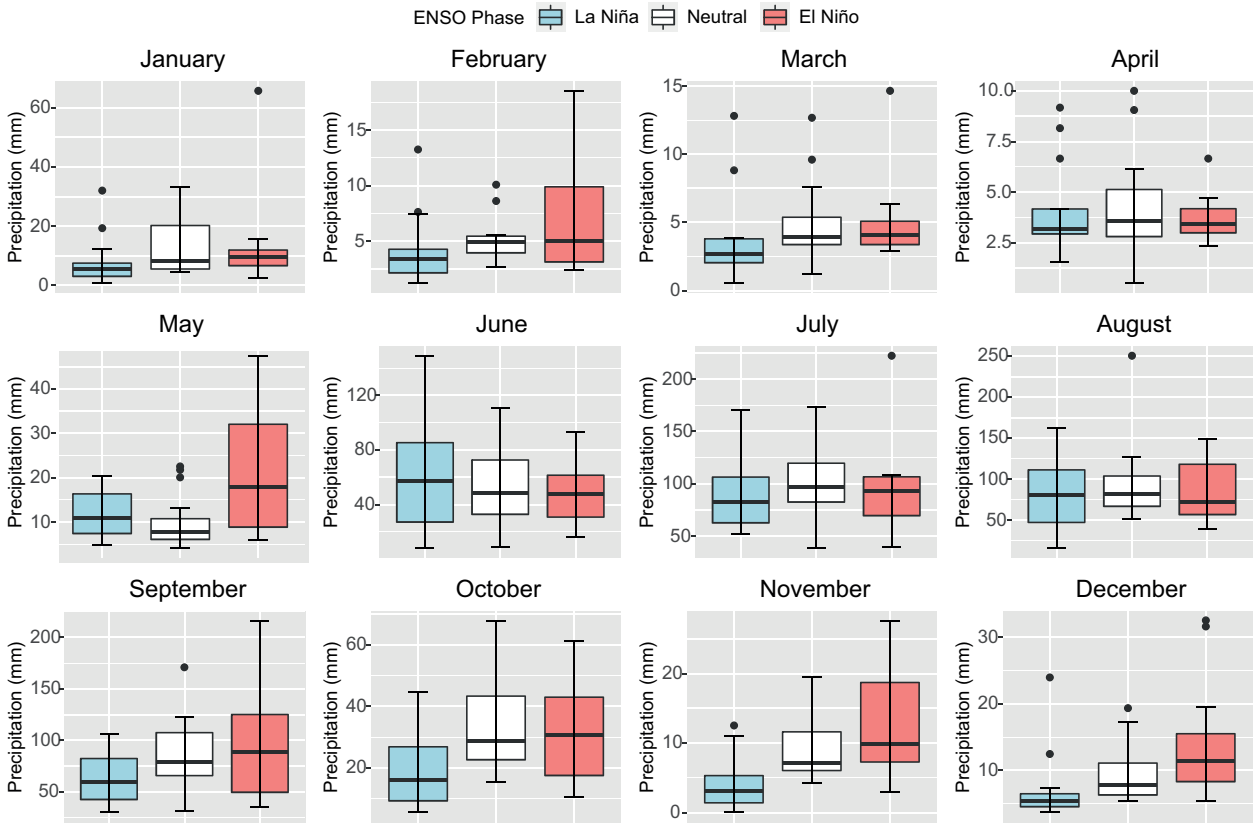

Fig. S2. Same as in Fig. S1 but for the Middle Nazas watershed.

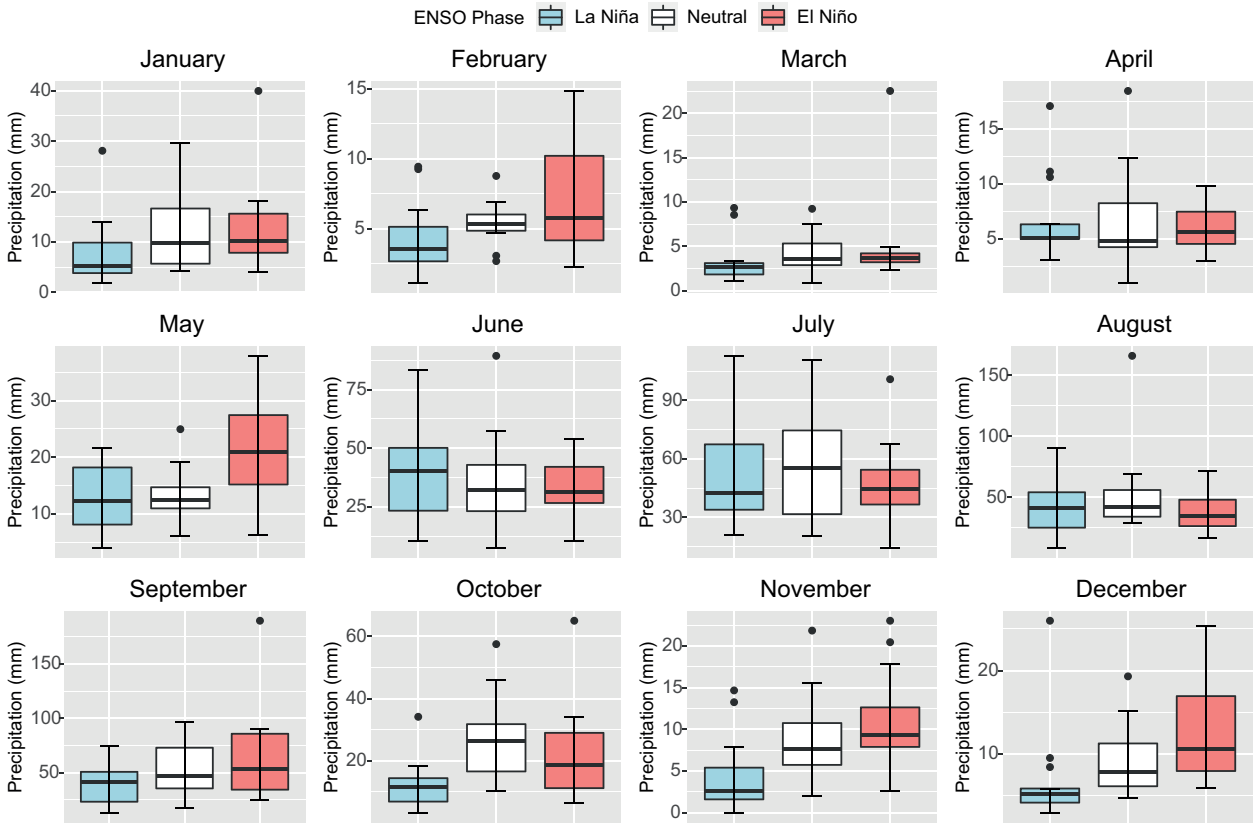

Fig. S3. Same as in Fig. S1 but for the Lower Nazas watershed.

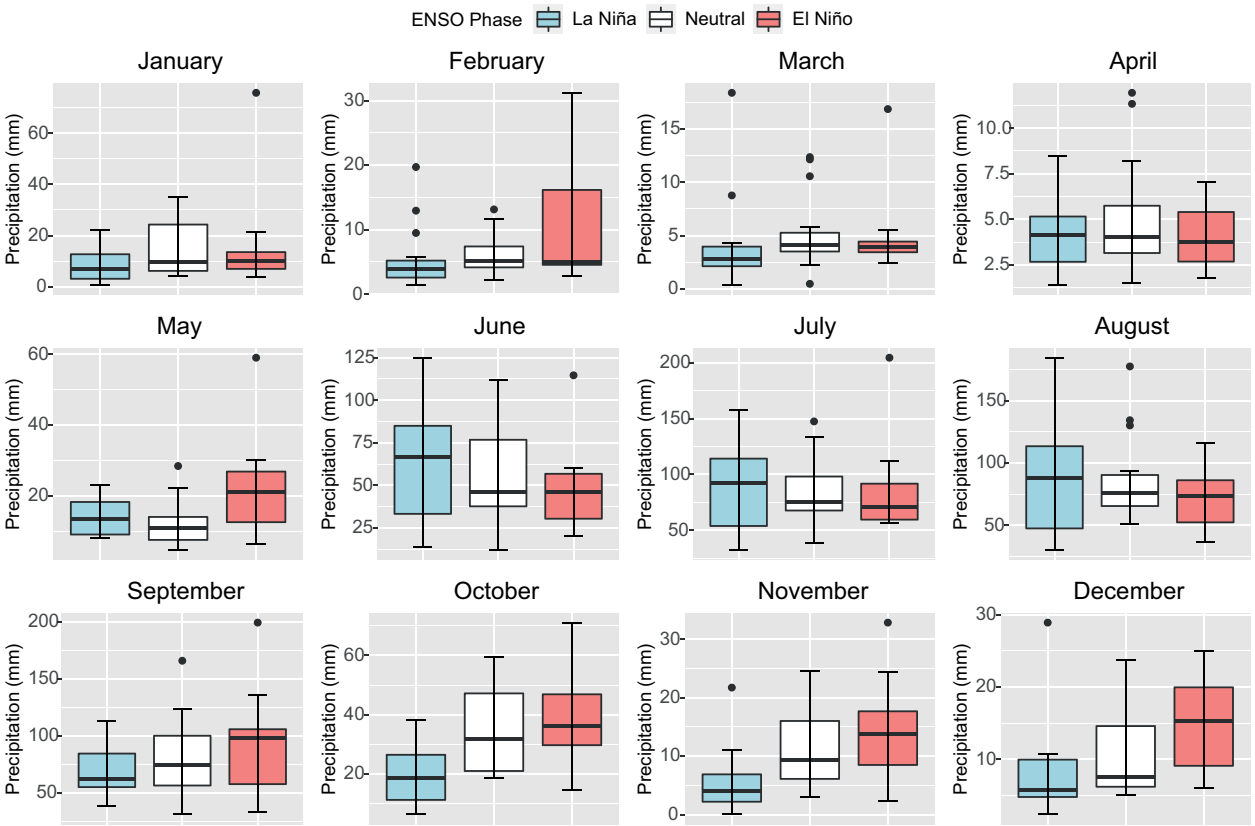

Fig. S4. Same as in Fig. S1 but for the Upper Aguanaval watershed.

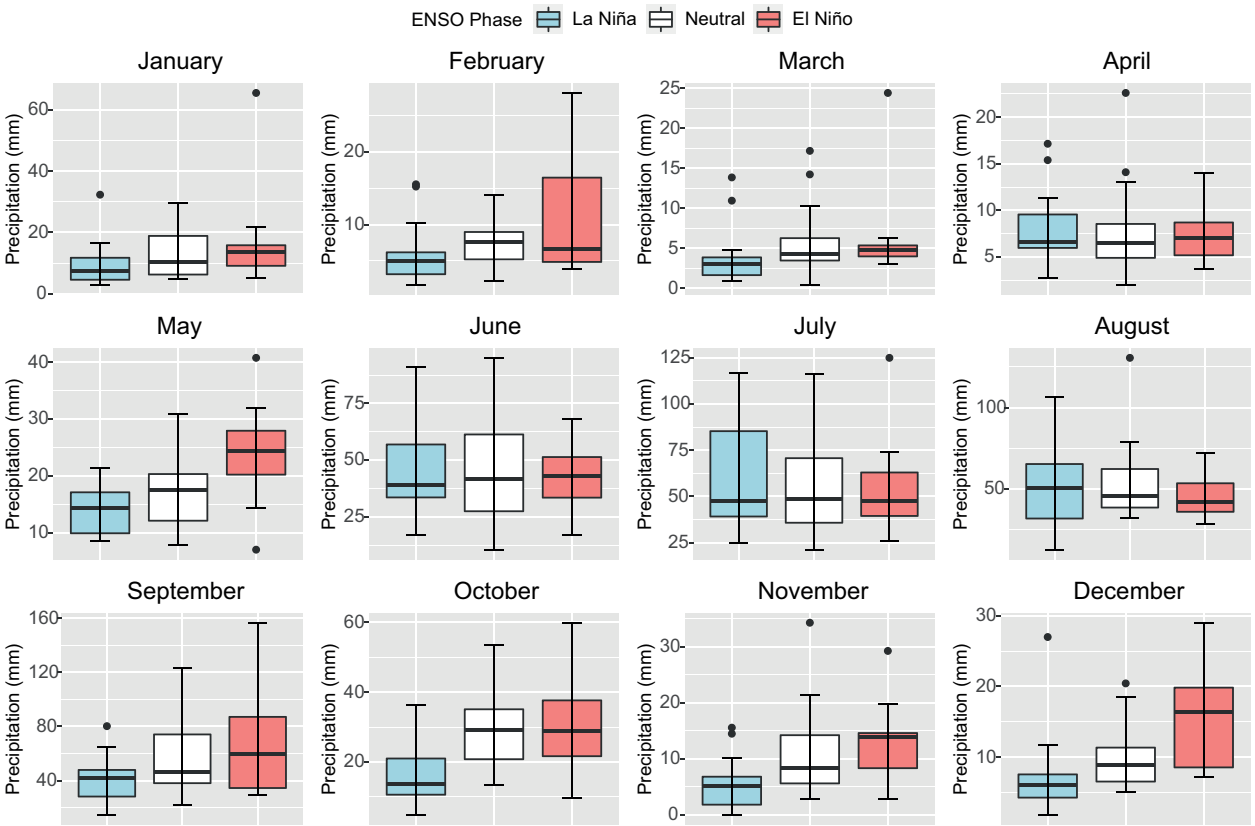

Fig. S5. Same as in Fig. S1 but for the Lower Aguanaval watershed.

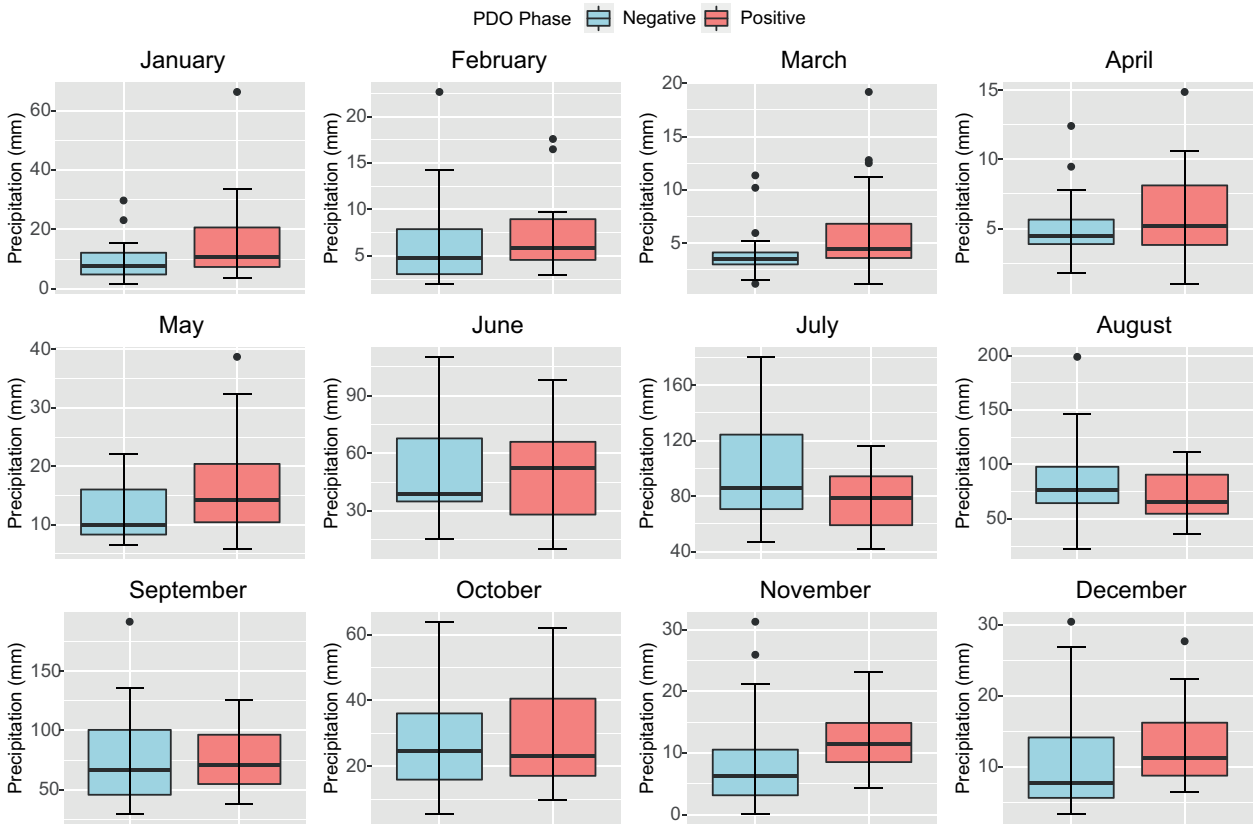

Fig. S6. Box and whisker plot for the PDO effect on monthly precipitation in the Nazas-Aguanaval watershed (1981-2021). The black center line denotes the median value (50th percentile); the black box encompasses the 25th to 75th percentiles of the dataset; whiskers indicate the 25th percentile + 1.5 times the interquartile range (IQR) and the 75th percentile +1.5 IQR, and black dots indicate the outliers.

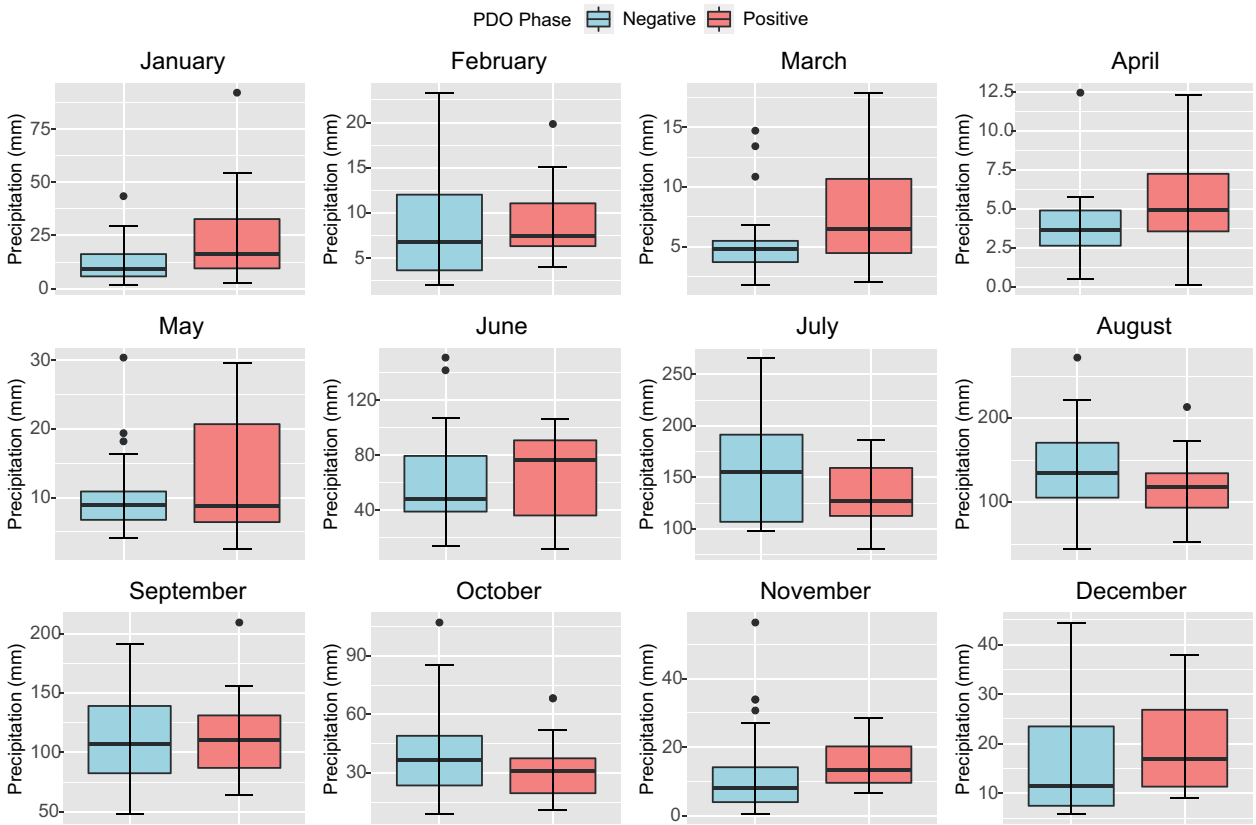

Fig. S7. Same as in Fig. S6 but for the Upper Nazas watershed (1981-2021).

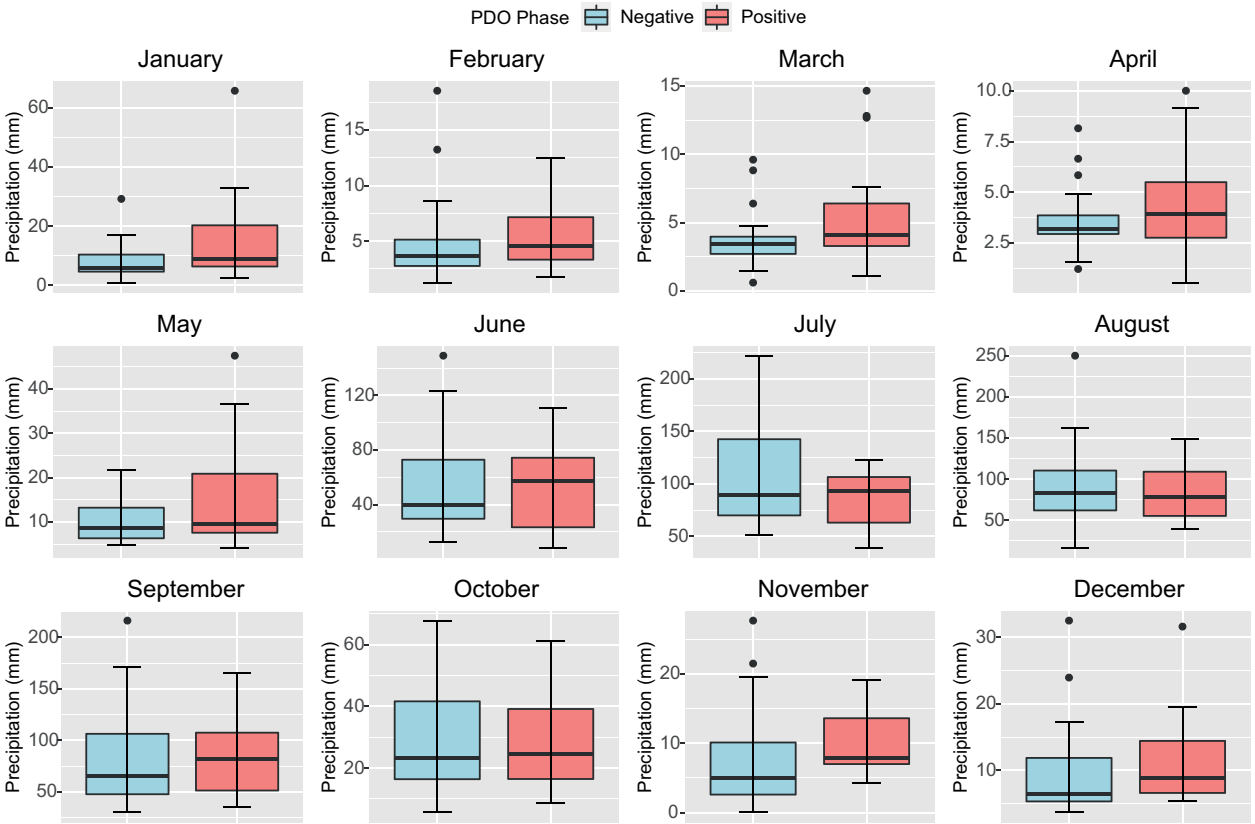

Fig. S8. Same as in Fig. S6 but for the Middle Nazas watershed (1981-2021).

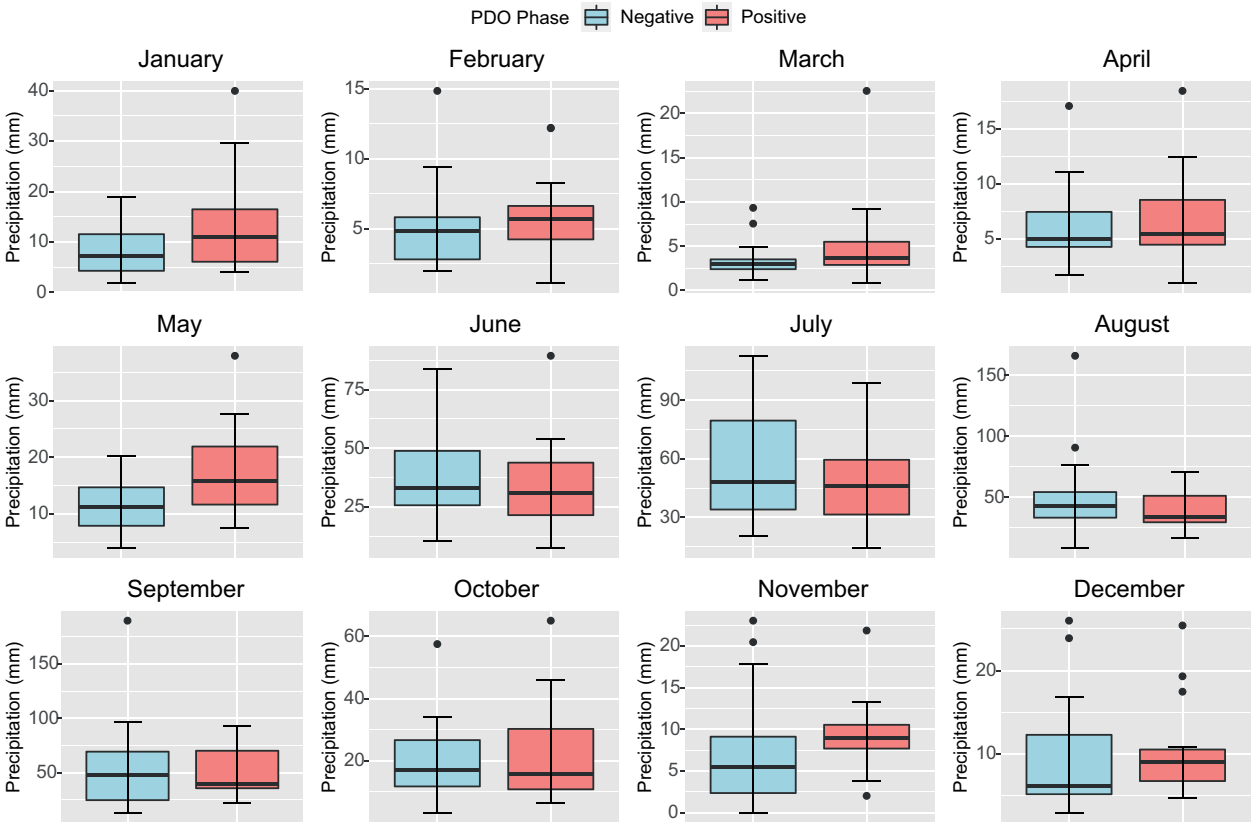

Fig. S9. Same as in Fig. S6 but for the Lower Nazas watershed (1981-2021).

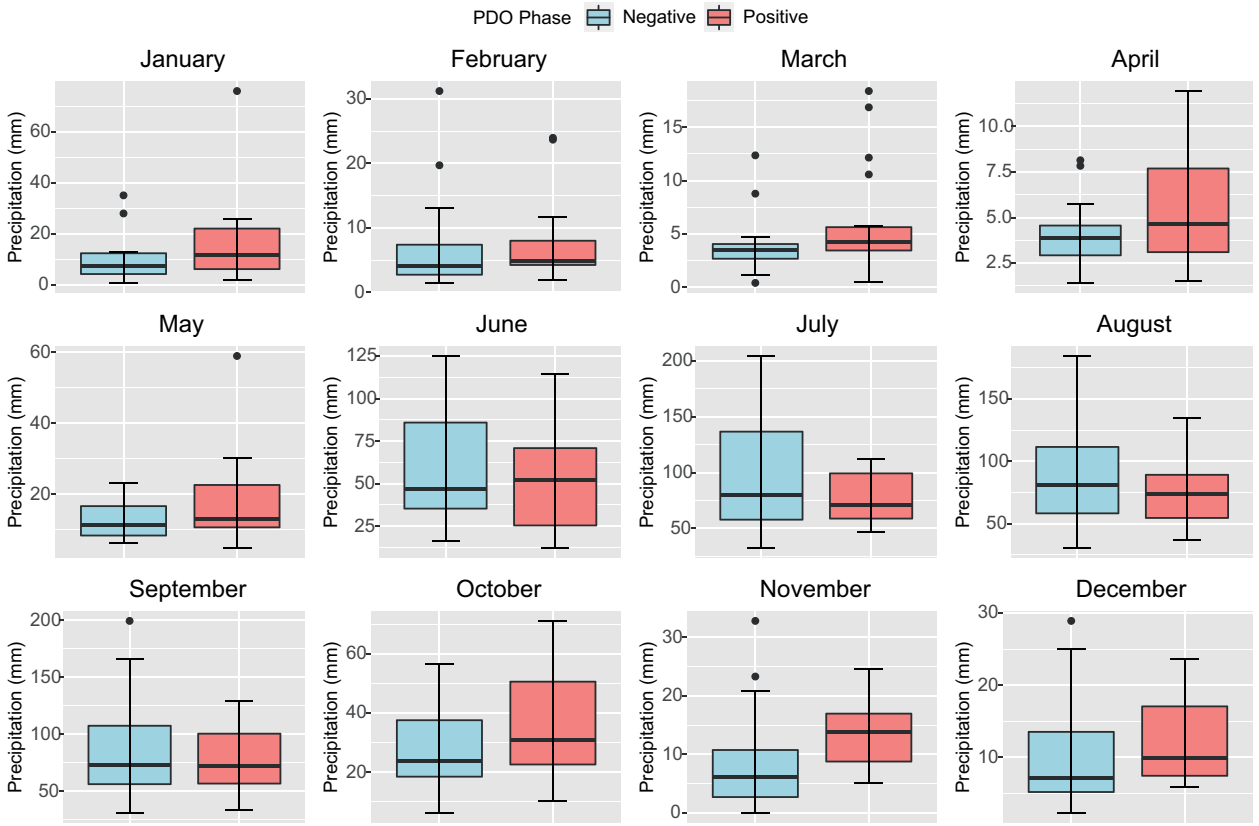

Fig. S10. Same as in Fig. S6 but for the Upper Aguanaval watershed (1981-2021).

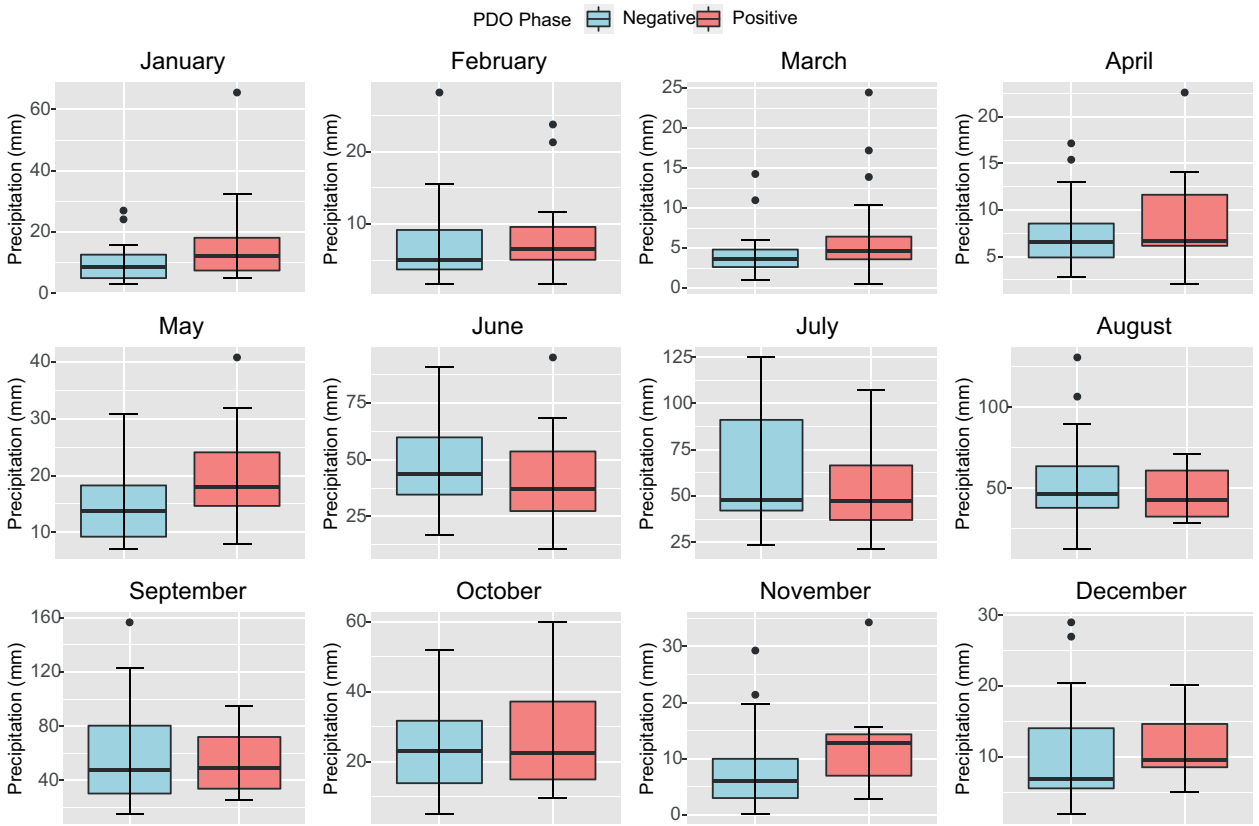

Fig. S11. Same as in Fig. S6 but for the Lower Aguanaval watershed (1981-2021).

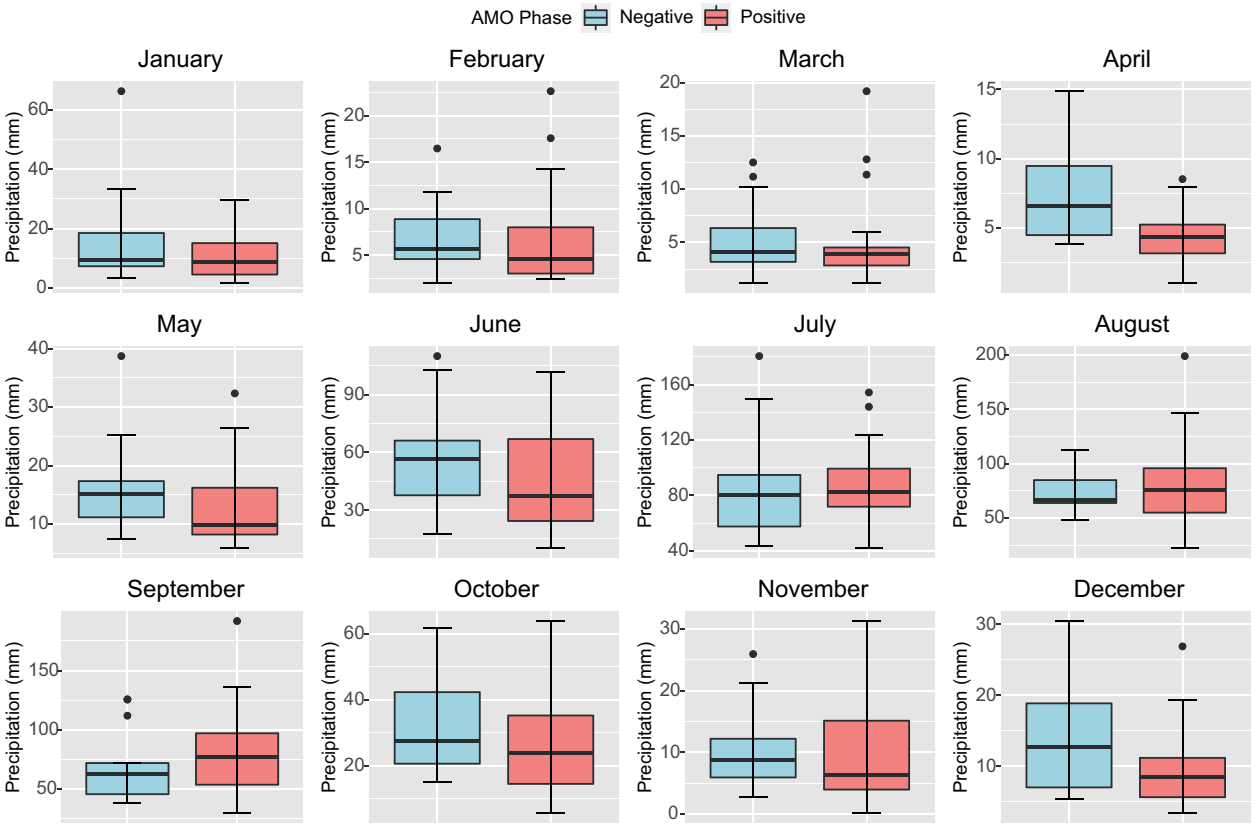

Fig. S12. Box and whisker plot for AMO effect on monthly precipitation in the Nazas-Aguanaval watershed (1981-2021). The black center line denotes the median value (50th percentile); the black box encompasses the 25th to 75th percentiles of the dataset; whiskers indicate the 25th percentile + 1.5 times the interquartile range (IQR) and the 75th percentile +1.5 IQR, and black dots indicate the outliers.

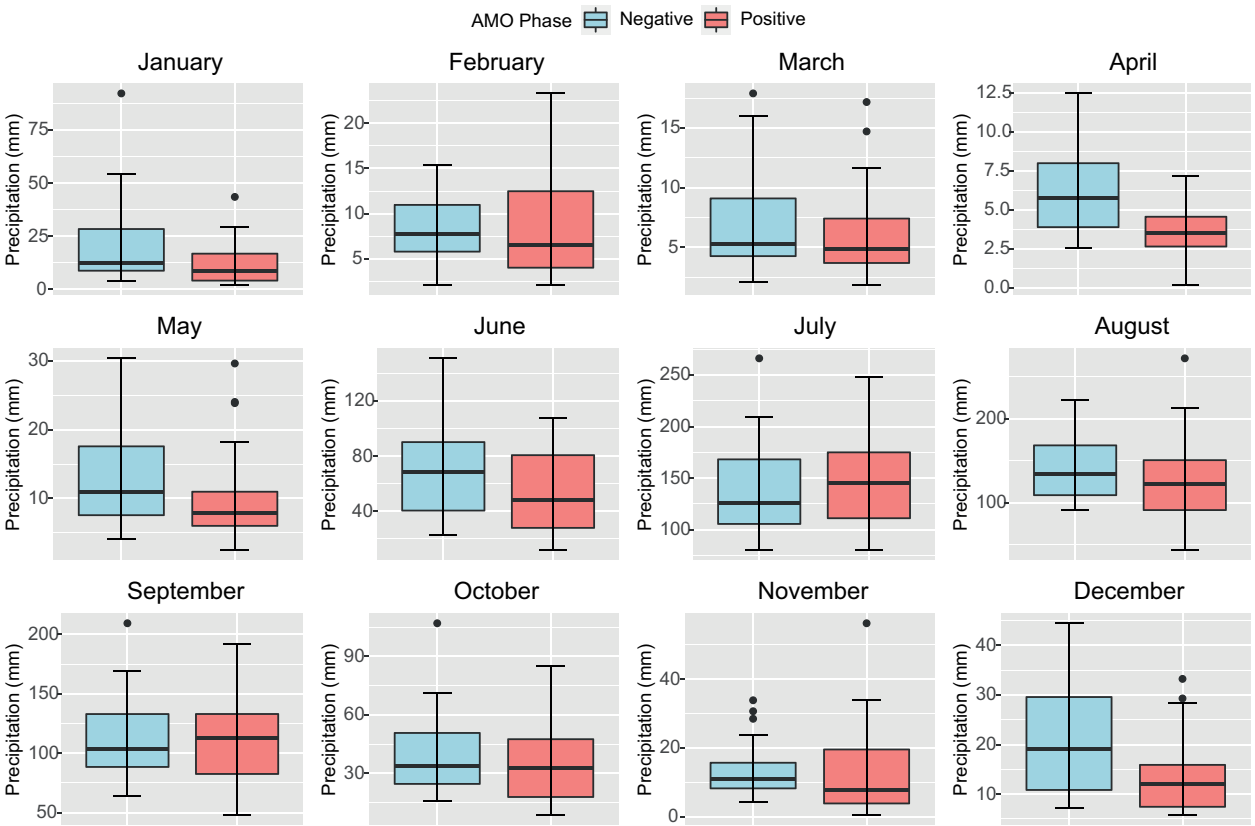

Fig. S13. Same as in Fig. S12, but for the Upper Nazas watershed (1981-2021).

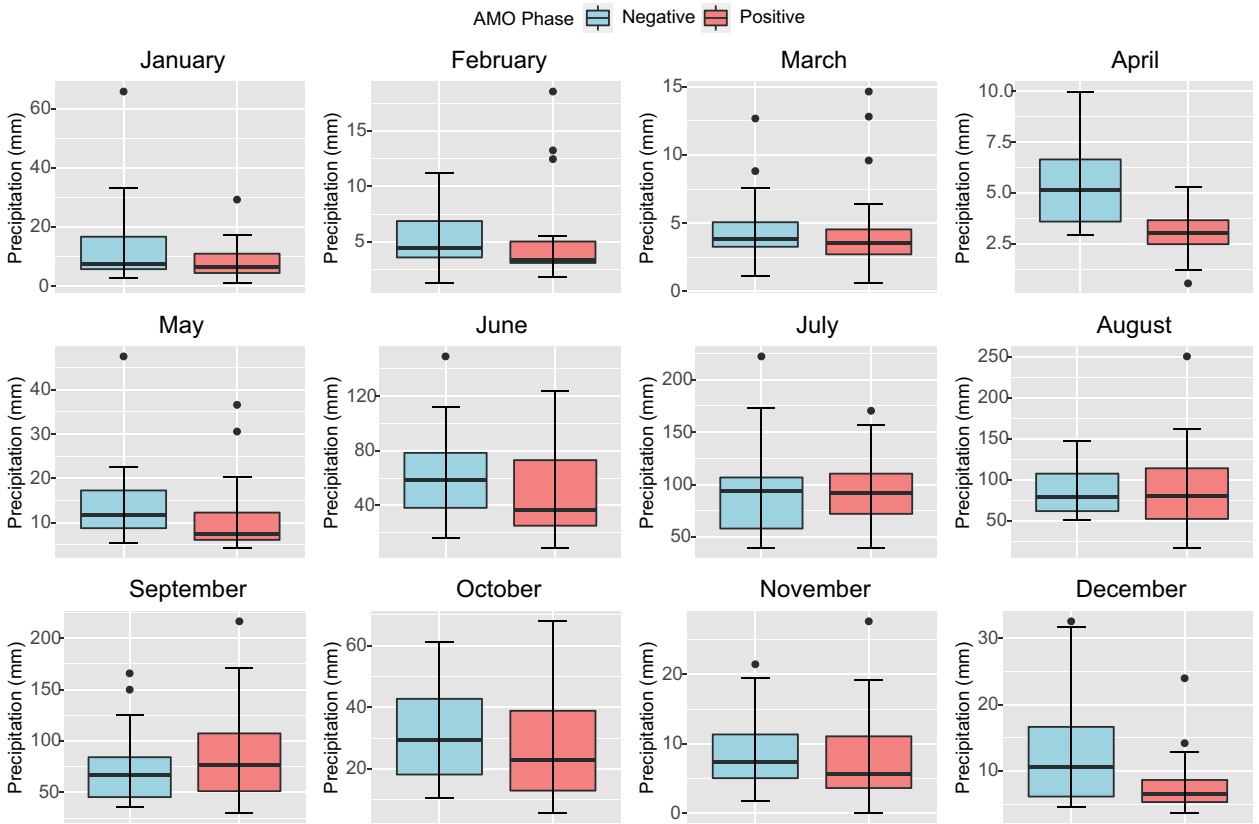

Fig. S14. Same as in Fig. S12, but for the Middle Nazas watershed (1981-2021).

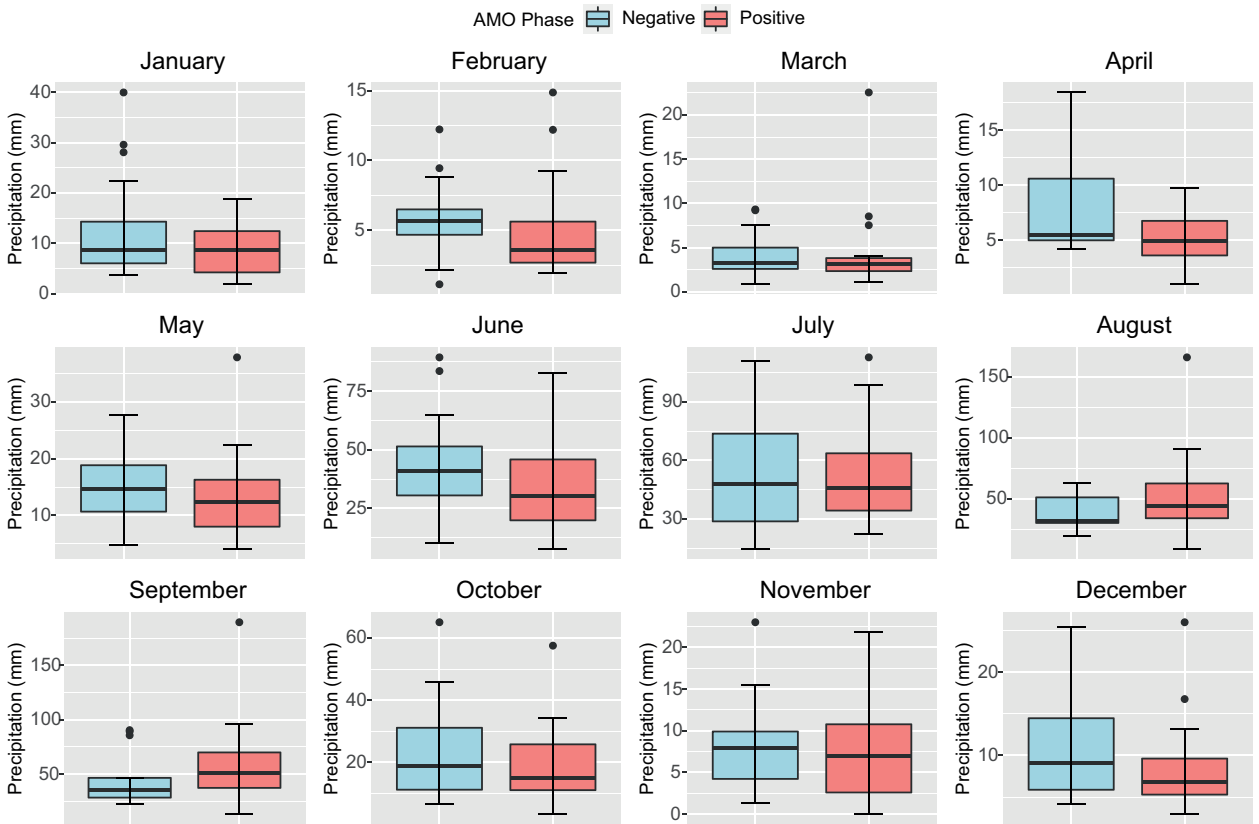

Fig. S15. Same as in Fig. S12, but for the Lower Nazas watershed (1981-2021).

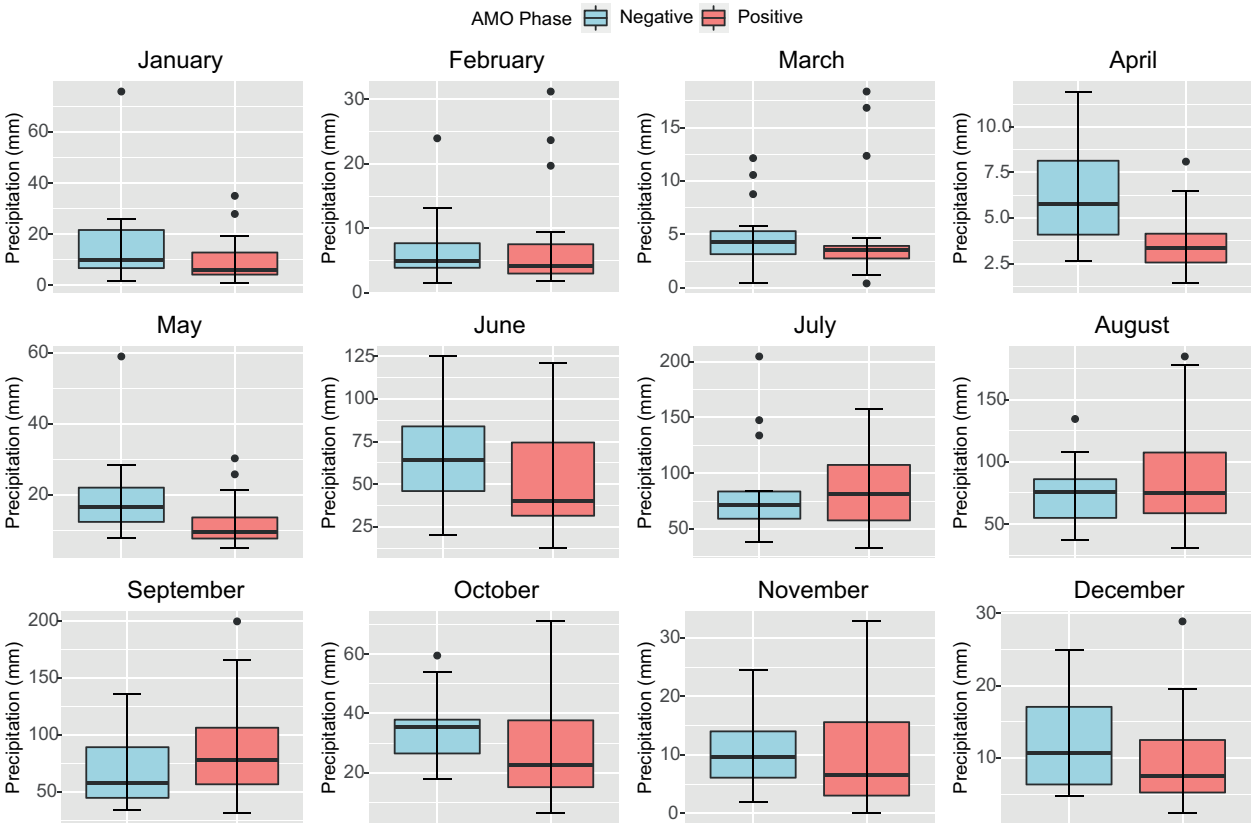

Fig. S16. Same as in Fig. S12, but for the Upper Aguanaval watershed (1981-2021).

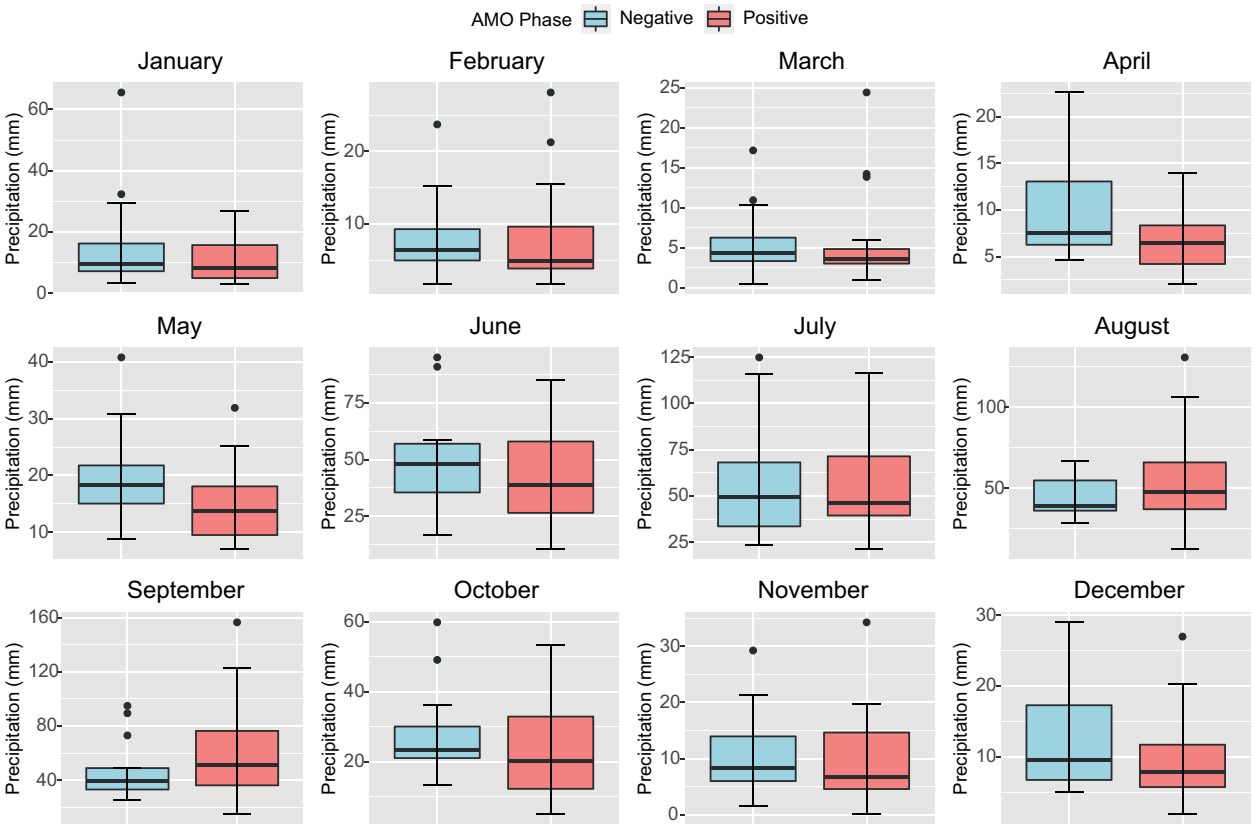

Fig. S17. Same as in Fig. S12, but for the Lower Aguanaval watershed (1981-2021).

Table SI. ANOVA p-values for ENSO influence on precipitation in the Nazas-Aguanaval watershed.

Month	Full watershed	Upper Nazas	Middle Nazas	Lower Nazas	Upper Aguanaval	Lower Aguanaval
January	**0.0308**	**0.0481**	0.0557	**0.0173**	0.0573	**0.0188**
February	**0.0141**	**0.0232**	**0.0160**	**0.0113**	**0.0247**	**0.0123**
March	0.0506	0.0548	**0.0482**	**0.0498**	0.2030	0.0661
April	0.8371	0.9601	0.8639	0.7033	0.8807	0.8025
May	0.1236	0.4734	0.2900	**0.0218**	0.3301	**0.0131**
June	0.3150	0.1847	0.6435	0.5265	0.3695	0.8943
July	0.8589	0.8703	0.8742	0.6884	0.8468	0.5574
August	0.9607	0.7593	0.6633	0.9439	0.6066	0.8746
September	0.1054	0.2057	0.1121	**0.0459**	0.2128	**0.0210**
October	**0.0183**	0.1895	**0.0246**	**0.0116**	**0.0014**	**0.0027**
November	**0.0001**	**0.0006**	**0.0000**	**0.0002**	**0.0003**	**0.0009**
December	**0.0002**	**0.0002**	**0.0005**	**0.0004**	**0.0013**	**0.0002**

Numbers in bold indicate statistical significance ($\alpha = 0.05$).

Table SII. ANOVA p-values for PDO influence on precipitation in the Nazas-Aguanaval watershed.

Month	Full watershed	Upper Nazas	Middle Nazas	Lower Nazas	Upper Aguanaval	Lower Aguanaval
January	**0.0236**	**0.0418**	**0.0291**	**0.0237**	0.0515	**0.0301**
February	0.2092	0.2501	0.2286	0.4519	0.2596	0.2970
March	0.0996	0.0841	0.1082	0.1247	0.1144	0.1767
April	0.3911	0.1056	0.2825	0.8367	0.1439	0.7132
May	0.0730	0.6759	0.3625	**0.0035**	0.3247	**0.0177**
June	0.6751	0.7067	0.8303	0.3111	0.4539	0.2427
July	0.1210	0.1115	0.1390	0.1887	0.3396	0.2084
August	0.4276	0.2740	0.7499	0.5369	0.4585	0.5125
September	0.8212	0.6638	0.5805	0.6197	0.5365	0.9385
October	0.6957	0.4861	0.8931	0.6054	0.1124	0.3709
November	0.0571	0.1234	0.0597	0.0966	**0.0111**	0.0546
December	0.1096	0.0743	0.1369	0.1524	0.1464	0.1916

Numbers in bold indicate statistical significance ($\alpha = 0.05$).

Table S3. ANOVA p-values for AMO influence on precipitation in the Nazas-Aguanaval watershed.

Month	Full watershed	Upper Nazas	Middle Nazas	Lower Nazas	Upper Aguanaval	Lower Aguanaval
January	0.1170	0.0560	0.0917	0.1362	0.2253	0.1914
February	0.5342	0.5681	0.8362	0.3375	0.9358	0.6224
March	0.5523	0.3583	0.5763	0.5879	0.6604	0.7999
April	**0.0013**	**0.0006**	**0.0001**	**0.0137**	**0.0001**	**0.0144**
May	**0.0251**	0.2099	**0.0425**	0.2279	**0.0066**	**0.0255**
June	0.1154	0.1859	0.0721	0.0611	0.1608	0.1763
July	0.6740	0.7031	0.8912	0.6988	0.7505	0.8033
August	0.8867	0.6223	0.9862	0.3116	0.7231	0.3284
September	0.4865	0.7463	0.7176	0.3648	0.1584	0.4363
October	0.2010	0.2682	0.2139	0.2778	0.1719	0.2037
November	0.4123	0.2421	0.3466	0.5236	0.3613	0.5824
December	0.0504	**0.0284**	**0.0155**	0.1513	0.1277	0.1726

Numbers in bold indicate statistical significance ($\alpha = 0.05$).